

---

Masters Theses

Student Theses and Dissertations

---

Fall 2018

## Salt mobility under different geological regimes

Oznur Surek

Follow this and additional works at: [https://scholarsmine.mst.edu/masters\\_theses](https://scholarsmine.mst.edu/masters_theses)



Part of the [Geophysics and Seismology Commons](#)

Department:

---

### Recommended Citation

Surek, Oznur, "Salt mobility under different geological regimes" (2018). *Masters Theses*. 7837.  
[https://scholarsmine.mst.edu/masters\\_theses/7837](https://scholarsmine.mst.edu/masters_theses/7837)

This thesis is brought to you by Scholars' Mine, a service of the Missouri S&T Library and Learning Resources. This work is protected by U. S. Copyright Law. Unauthorized use including reproduction for redistribution requires the permission of the copyright holder. For more information, please contact [scholarsmine@mst.edu](mailto:scholarsmine@mst.edu).

SALT MOBILITY UNDER DIFFERENT GEOLOGICAL REGIMES

by

OZNUR SUREK

A THESIS

Presented to the Graduate Faculty of the

MISSOURI UNIVERSITY OF SCIENCE AND TECHNOLOGY

In Partial Fulfillment of the Requirements for the Degree

MASTER OF SCIENCE

in

GEOLOGY AND GEOPHYSICS

2018

Approved by

Dr. Kelly Liu

Dr. Stephen Gao

Dr. Neil Anderson

Copyright 2018  
OZNUR SUREK  
All Rights Reserved

## ABSTRACT

This study investigates the evolution of Dan Salt Structure in the southern salt dome province, Danish Central Graben and Mars-Ursa Basin in the Northern Gulf of Mexico to understand salt and sediment interaction over time under different geologic regimes. An integration of structural and stratigraphic analyses is conducted to understand the relationship between halokinesis and sedimentation.

Interpretation of the seismic data in Dan Salt Structure shows that the structure has a complex geometry, which is divided into upper and lower parts. The evolutionary stage of both the upper and lower parts of the structure has been influenced by salt. The structure is determined as a wall-and-sill complex that relates extensional tectonics and is interpreted as an asymmetric roller-type salt structure within the NNW-SSE fault. Interpretation of the seismic data in Mars-Ursa Basin shows that the basin is a salt withdrawal minibasin and surrounded by Allochthonous salt bodies. The seismic data covers two salt bodies, namely, Salt Body A and Salt Body B. Active salt diapirism was observed at the eastern edge of Salt Body A. Active diapirism shows elongation in N-S direction and is accompanied by growth faulting. Gas hydrate related to active diapirism and faulting is also recognized above Salt Body A. Reactive salt diapirism is observed at the eastern edge of Salt Body B. Reactive diapirism shows elongation in the E-W direction and accompanied by normal faulting.

Although the Northern Gulf of Mexico and Danish Central Graben has different geological history, both the Dan Salt Structure and the Mars-Ursa Basin went through regional extension locally. It is known that there is direct relation between diapirism and regional extension. While the Mars-Ursa Basin represents active and reactive salt diapirism, the Dan Salt structure represents a wall-and-sill complex. A possible reason why Dan Salt Structure did not become diapiric is the allochthonous movement in the Triassic strata.

## ACKNOWLEDGMENTS

I would like to express my deep gratitude to my advisor, Dr. Kelly Liu, for her encouragement, and patient guidance. I appreciate the countless time she has spent helping me.

I would like to thank my committee members, Dr. Stephen Gao and Dr. Neil Anderson, for their help, and suggestions in completing my study.

This work was not possible without my sponsor, Turkish Petroleum Corporation. I am gratefully indebted to my sponsor for giving me such a unique opportunity.

I would like to acknowledge to Geological Survey of Denmark and Greenland and Bureau of Ocean Energy Management for providing the seismic data set.

Finally, I would like to thank my parents whom my longing to be with them was one of the motivation for me to finish this thesis.

## TABLE OF CONTENTS

|  | Page |
|--|------|
| ABSTRACT .....   | iii  |
| ACKNOWLEDGMENTS .....                                      | iv   |
| LIST OF ILLUSTRATIONS .....                                | viii |
| LIST OF TABLES .....                                       | xi   |
| <br>SECTION  |      |
| 1. INTRODUCTION.....                                       | 1    |
| 2. THE DAN SALT STRUCTURE .....                            | 2    |
| 2.1. AREA OVERVIEW.....                                    | 2    |
| 2.2. EVOLUTION OF THE PERMIAN BASIN (ZECHTEIN BASIN) ..... | 3    |
| 2.3. THE CENTRAL GRABEN .....                              | 4    |
| 2.4. THE DANISH CENTRAL GRABEN .....                       | 7    |
| 2.5. THE SOUTHERN SALT DOME PROVINCE .....                 | 9    |
| 2.6. SALT STRUCTURES .....                                 | 9    |
| 2.7. FAULT SYSTEM IN THE DANISH SALT DOME PROVINCE .....   | 10   |
| 2.7.1. The Coffee Soil Fault.....                          | 10   |
| 2.7.2. Dan Transverse Zone .....                           | 12   |
| 2.8. SALT MOBILIZATION AND FAULT RELATIONSHIP .....        | 13   |
| 3. THE MARS-URSA BASIN .....                               | 16   |
| 3.1. AREA OVERVIEW.....                                    | 16   |

|      |  |    |
|------|--|----|
| 3.2. | THE GULF OF MEXICO BASIN .....                 | 16 |
| 3.3. | THE MISSISSIPPI CANYON .....                   | 18 |
| 3.4. | THE MARS-URSA BASIN .....                      | 18 |
| 3.5. | MINIBASINS .....                               | 18 |
| 3.6. | SALT STRUCTURE .....                           | 19 |
| 3.7. | SALT MOBILIZATION AND FAULT RELATIONSHIP ..... | 20 |
| 4.   | SALT TECTONICS .....                           | 22 |
| 4.1. | INTRODUCTION OF SALT .....                     | 22 |
| 4.2. | DIAPIRISM .....                                | 24 |
| 4.3. | ALLOCHTHONOUS SALT .....                       | 26 |
| 5.   | DATA AND METHODOLOGY .....                     | 27 |
| 5.1. | SEISMIC DATA .....                             | 27 |
| 5.2. | METHODOLOGY .....                              | 29 |
| 6.   | SEISMIC ATTRIBUTES .....                       | 30 |
| 6.1. | VARIANCE .....                                 | 30 |
| 6.2. | RMS AMPLITUDE.....                             | 36 |
| 7.   | SEISMIC INTERPRETATION .....                   | 39 |
| 7.1. | FAULT INTERPRETATION .....                     | 39 |
| 7.2. | SALT INTERPRETATION .....                      | 42 |
| 8.   | RESULTS .....                                  | 47 |
| 8.1. | DAN SALT STRUCTURE .....                       | 47 |
| 8.2. | MARS-URSA BASIN .....                          | 54 |

|                     |    |
|---------------------|----|
| 9. CONCLUSIONS..... | 64 |
| BIBLIOGRAPHY.....   | 66 |
| VITA.....           | 72 |



## LIST OF ILLUSTRATIONS

| Figure  | Page |
|---|------|
| 2.1 Location map and structural elements of the Danish Central Graben. The study area is outlined in red (Sundsbø and Megson, 1993). . . . .  | 3    |
| 2.2 Map of the Permian sedimentary basin in northwest Europe. The Southern salt dome province was located at Southern Permian Basin (after Evans et al., 2003). . . . .   | 5    |
| 2.3 Location map of the Danish Central Graben in respect to the Danish North Sea. The study area is outlined in red (Vejbæk and Kristensen, 2000). . . . .  | 8    |
| 2.4 Stratigraphic framework shown ages and representative lithologies of the formations presented in the Danish Central Graben with the major tectonic events (Duffy et al., 2013). . . . .   | 11   |
| 2.5 Danish Central Graben structural elements with faults at the Base Chalk level. Oil and gas fields with chalk reservoirs are also shown. The study area is outlined in red. Modified from (Klinkby et al., 2005). . . . .                              | 13   |
| 2.6 Schematic cross sections shown the influence of the ductile salt layer on the rift structural style and stratal geometry style during rifting phase (Duffy et al., 2013). . . . .   | 15   |
| 3.1 Location map of the Mississippi Canyon. The study area is outlined in red (Bouroullec et al., 2004). . . . .  | 17   |
| 3.2 Diagram shown Deposition of the salt. A.) Initial Jurassic pre-rift position of Yucatan Peninsula; B.) Jurassic rotation, continental crust extension and seafloor spreading; C.) Rotation and present position achieved (Bird et al., 2005). . . . . | 21   |
| 4.1 Schematic shapes of salt structures (Fossen, 2010). . . . .   | 23   |
| 4.2 Models of diapir piercement in schematic cross sections (Hudec and Jackson, 2007). . . . .  | 25   |
| 5.1 Base map of the Dan Field. . . . .  | 27   |
| 5.2 Base map of the Mars-Ursa Field. . . . .  | 28   |
| 6.1 Time slice at 2.012 s from the Dan Field. Faults and channel system are invisible. . . . .  | 31   |
| 6.2 Variance attribute time slice at 2.012 s from the Dan Filed shown uninterpreted faults and channel system. . . . .  | 32   |

|     |   |    |
|-----|---|----|
| 6.3 | Variance attribute time slice at 2.012 s from the Dan Filed shown interpreted faults and channel system. Faults and channel system visibility is significantly improved. ....   | 33 |
| 6.4 | Time slice at 2.066 s from the Mars-Ursa Basin. Salt structures and minibasins are invisible. ....  | 34 |
| 6.5 | Variance attribute time slices. A.) Variance attribute time slice at 2.066 s from the Mars-Ursa Basin. Salt structures and minibasins visibility is significantly improved. B.) Variance attribute time slice at 2.066 s shown interpreted salt structures and minibasins. ....                         | 35 |
| 6.6 | Vertical seismic section of Crossline 765 shown with gas chimney, salt body, and unconformity. ....   | 37 |
| 6.7 | RMS amplitude attribute window shows bright spots, gas chimney, salt body, and unconformity in Crossline 765 from the Mars-Ursa Field. Shallow high amplitude events related to the presence of gas and different packages of lithologies are easily identified in RMS amplitude attribute window. .... | 38 |
| 7.1 | Three-dimensional visulation of interpreted major and minor faults. A.) Three-dimensional visulation of interpreted faults in Mars-Ursa Filed. B.) Three-dimensional visulation of interpreted faults in Dan Filed. ....  | 40 |
| 7.2 | Vertical seismic section of Crossline 478 shown with interpreted faults. Green fault represents NW-SE trending Dan Transverse Zone. ....  | 41 |
| 7.3 | Three-dimensional visualization of salt distributions. Salt ridge of interpreted salt bodies in the Dan field. ....   | 43 |
| 7.4 | Vertical seismic section of the Inline 322 shown interpreted salt bodies and faults. ....   | 44 |
| 7.5 | Three-dimensional visualization of salt distributions. Salt ridge of two interpreted salt bodies in the Mars-Ursa field. ....   | 45 |
| 7.6 | Vertical seismic section of the Inline 48100 shown interpreted salt bodies and faults. ....   | 46 |
| 8.1 | Vertical seismic section of Inline 772 shown uninterpreted salt bodies and faults. ....   | 48 |
| 8.2 | Vertical seismic section of Inline 772 shown interpreted salt bodies, faults, and salt roller type salt structure. ....   | 49 |
| 8.3 | Vertical seismic section of Inline 329 shown uninterpreted salt bodies and faults. ....   | 52 |
| 8.4 | Vertical seismic section of Inline 329 shown interpreted salt bodies and faults. ...  | 53 |
| 8.5 | Vertical seismic section of Inline 201 shown uninterpreted salt bodies and faults. ....   | 55 |

|      |   |    |
|------|---|----|
| 8.6  | Vertical seismic section of Inline 201 shown interpreted salt bodies and faults...                  | 56 |
| 8.7  | Vertical seismic section of Inline 47000 shown interaction between salt bodies and minibasins. .... | 58 |
| 8.8  | Vertical seismic section of Inline 4573 shown uninterpreted salt body and faults.                   | 60 |
| 8.9  | Vertical seismic section of Inline 4573 shown interpreted reactive diapirism and faults. ....       | 61 |
| 8.10 | Vertical seismic section of Crossline 765 shown uninterpreted salt body and faults. ....            | 62 |
| 8.11 | Vertical seismic section of Crossline 765 shown interpreted active diapirism and faults. ....       | 63 |

**LIST OF TABLES**

| Table   | Page |
|---|------|
| 4.1 Summarized information of salt properties. .... | 24   |

## 1. INTRODUCTION

Rock salt has its own physical and chemical properties, such as plastic rheology and low mechanical strength, low density and compressibility, and exceptionally high solubility. It is well known that rock salt has a major influence on the structural styles in sedimentary packages, which is known as overburden, above salt structures and even on undeformed salt layer (Fossen, 2010). The majority of the explored hydrocarbon areas are found associated with salt basins in the Gulf of Mexico and the North Sea.

Rock salt exhibits low density around  $2.200 \text{ kg/m}^3$  and is almost incompressible material in respect to the surrounding overburden. This incompressibility causes density inversion at a certain depth, and salt becomes less dense than the overburden sediment. Consequently, salt flow and halokinetic movement occur. In salt related basins, halokinetic movements have significant roles to produce different tectonic styles, create structural traps, and control the distribution of reservoirs around the salt. The salt has the ability to create structure closures, play a role in reservoir distribution and heat conduction, and to act as a seal to fluid migration (Hudec and Jackson, 2007). For these reasons, understanding salt tectonics is significant for the hydrocarbon exploration.

Salt exhibits different structural style, and salt mobility differs from region to region. In order to understand the difference of salt mobility under different regional geology, two different salt related basins are examined through seismic study.

## 2. THE DAN SALT STRUCTURE

### 2.1. AREA OVERVIEW

The Dan Field is located in southwest part of the Danish North Sea (Figure 2.1). The field lies in the southern part of the North Sea Central Graben and is part of a trend of halokinetically derived structures in the southern salt dome province (Jorgensen, 1992). In the North Sea, the zechstein evaporites accumulated in the central graben during late Permian. Subsidence maintained during the Triassic time and mainly continental clastic and evaporitic sediment was accumulated. A tectonic Kimmeridgian pulse caused to deepening of the Central Graben at the time end of the Triassic (Møller and Rasmussen, 2003).

Afterwards, a shift in the depositional regime took place and altered from continental to predominantly marine or transitional environments with deposit of the thick shale sequences. Due to the differential movement of individual fault blocks, deposits varied across the Central Graben. Consequently, thickness difference in the Jurassic sequences occurred. The Permian salt, which started moving in the Triassic, was remobilized by the late Kimmeridgian tectonic pulse at end of the Jurassic time (Møller and Rasmussen, 2003).

As a result, many of salt pillows and salt diapirs in the south salt dome province was formed. The Dan Salt Structure is one of them. The dome was formed by uplifting a salt pillow on the Triassic age and subjected to various growth experiences from Late Jurassic to Late Tertiary. The significant growth at the Dan structure took place throughout the Eocene and followed by limited movements during Oligocene and Early Miocene. The structure is divided into two parts by a NE-SW trending normal fault, i.e., Dan Transverse Zone (Rank-friend and Elders, 2004) (Figure 2.1).

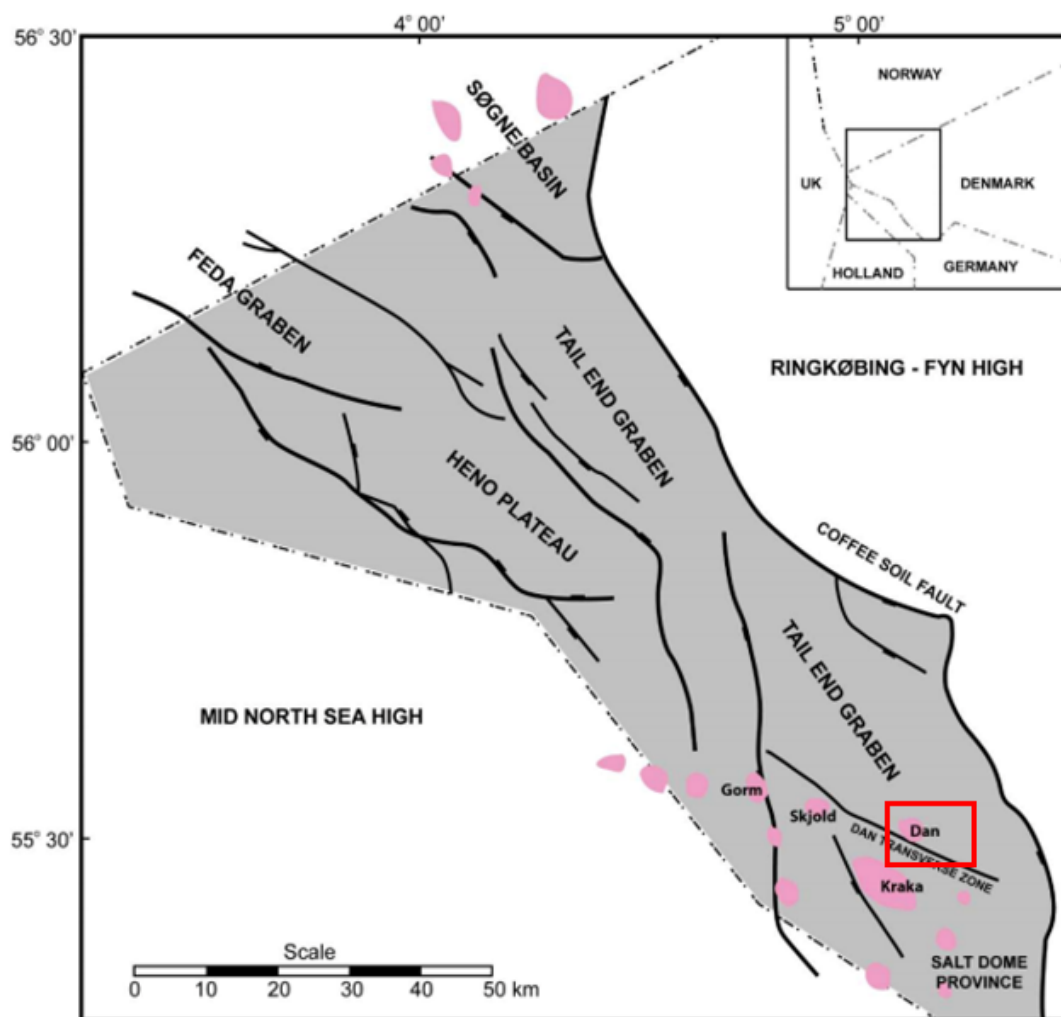


Figure 2.1. Location map and structural elements of the Danish Central Graben. The study area is outlined in red (Sundsbo and Megson, 1993).

## 2.2. EVOLUTION OF THE PERMIAN BASIN (ZECHEIN BASIN)

The Southern and the Northern Permian basins which extend across the present day southern North Sea and the Central North Sea were generated by two interconnected basins formed throughout the region of NW Europe (Figure 2.2).

The evolution of the Permian Basin is attributed by several processes mainly related to the late orogenic collapse of the Variscan mountain belt that formed through the suturing of Gondwanaland and Laurasia resulting in super continent Pangea. The continental rifting with thermal subsidence was followed by the Carboniferous extension (Glennie and Buller, 1983; Coward, 1995). These basins are flooded by the Rotliegend group Aelodian sediments of Early Permian age.

In the late Permian, thick salt formation (Zechstein group) was deposited as a consequence of flooding by the Boreal ocean somewhere close to Norway and Greenland along the preexisting fractures of the Proto Atlantic and North Sea fracture systems at these basins possibly due to a rise in sea level across the world. This sea level change occurred at the same time as the end of the Permian glaciation (Glennie, 1998; Zeigler, 1982).

The entrance route of Zechstein water into the Southern Permian Basin is argued with different theories. The Northern and Southern Permian basins had a connection with the graben system (e.g., Central Graben), which formed as a result of an active corridor between the basins. A previous study suggested a different route for flooding. The study assumes that until the Triassic time, the Central Viking Graben system did not exist (Zeigler, 1990). Considerably thick Rotliegend Aeolian Sabkha sand exists in the southern Viking Graben along with thick Zechstein halite, which is thick enough to behave as a diapiric. However, there is a graben that is in an initial stage already formed in the Zechstein flooding time (Glennie, 1998).

### **2.3. THE CENTRAL GRABEN**

The Central Graben is the southern arm of the North Sea Rift system that trends NNW-SSE. The Graben is located about 455 km from the area between UK and Norwegian continental shelves via the German and Danish sector to the Dutch sector.



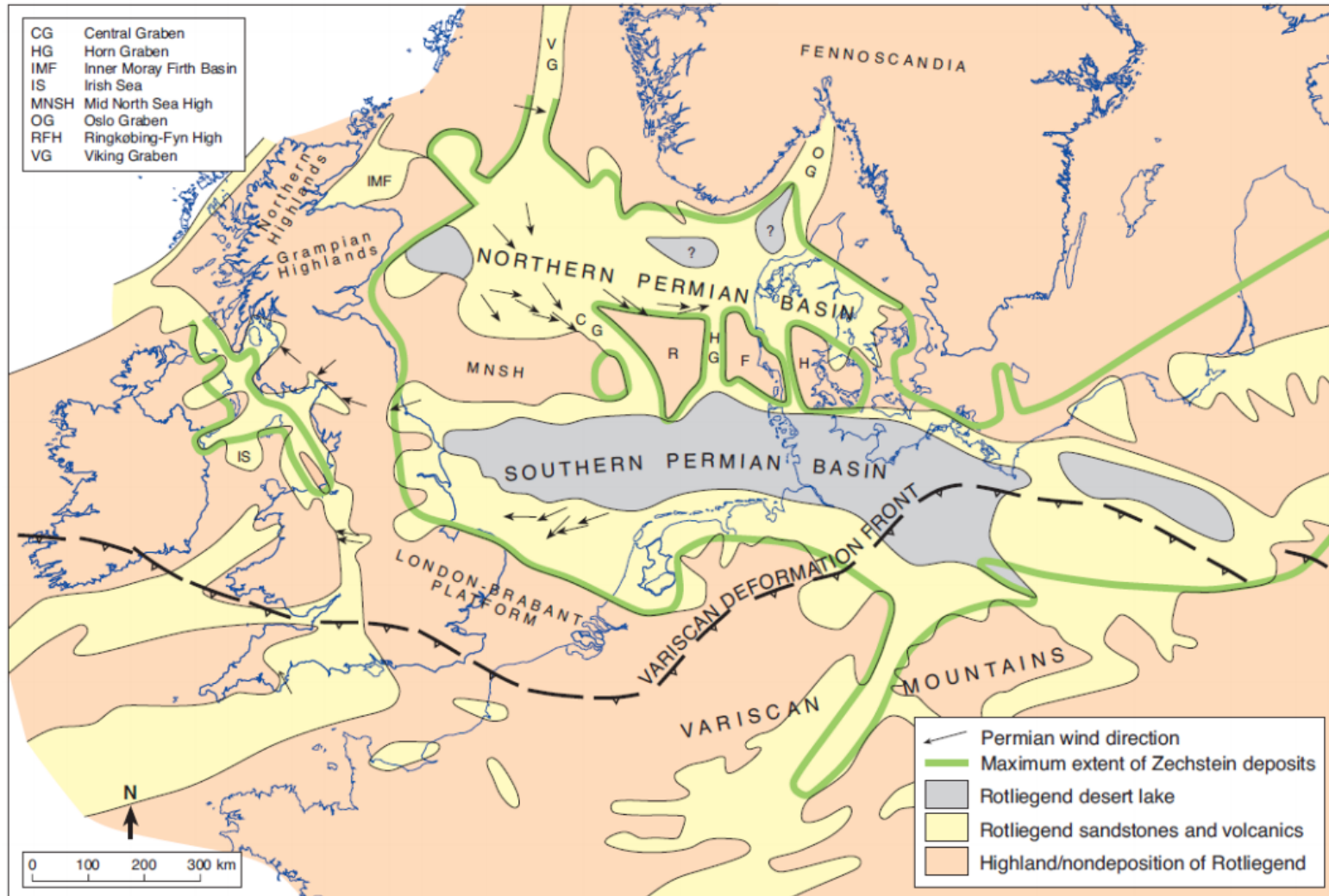


Figure 2.2. Map of the Permian sedimentary basin in northwest Europe. The Southern salt dome province was located at Southern Permian Basin (after Evans et al., 2003).

The Central Graben is traced back to the Permo-Triassic motion and followed by Late Jurassic motion. During the Triassic time, deformation in the North Sea was shaped by two main movements: extensional rifting (Zeigler, 1992) and mobilization of evaporites (Stewart and Clark, 1999).

The greater part of the Caledonian structural trend (Permian Basin and Mid North Sea High) was crosscut by the Triassic rift system, and new graben systems were formed, namely, the Viking and Central Graben. Permian Carboniferous fracture systems were also reactivated.

The Triassic rift system created deep half grabens in the eastern North Sea (Evans, 2003). Differential loading on thick sediment in the half graben causes to flow of the salt, the majority of the salt zones cannot keep their form and started to produce salt structures (Clark et al., 1999; Sundsbø and Megson, 1993).

Over the Mid-Jurassic, the Central North Sea was uplifted and a wide dome formed due to thermal heating. The Central Graben was distributed by this thermal dome and extended in E-W and N-S directions from Denmark to south Scotland and South Viking Graben into the North Sea (Zeigler and Horn, 1989).

Volcanic activity around the triple junction among the Central, Viking, and Moray Firth Grabens occurred due to thermal doming. As a consequence, structural relief took place (Zeigler and Horn, 1989). This uplifting of the Mid North Sea Thermal Dome ended with the extension of Triassic and Permian rocks and sedimentation in the Central Graben. The collapse of the thermal dome led to a new rifting stage in the Mid-Jurassic to Early Cretaceous (Møller and Rasmussen, 2003).

In the Late Jurassic, three extension events occurred. The first one was in the Late Aalenian to the Early Oxfordian, defined by the development of NNW-SSE to N-S striking faults. In the Late Kimmeridgian to Early Volganian, the second rifting occurred and kept

in thick deposits in the hanging wall of the NNW-SSE trending faults. The third extension took place during the Ryazanian and led to reactivation of the NNW-SSE striking faults (Møller and Rasmussen, 2003).

#### **2.4. THE DANISH CENTRAL GRABEN**

The Danish Central Graben is a major half graben system dipping eastward at the place that rifting system switches from NW-SE in the Norwegian and UK to N-S Dutch sector (Figure 2.3). The Mid-North Sea High was located at the western side of the Danish Central Graben. The Danish part of the Central Graben is divided into sub-basins diverged by intra-basinal highs.

Structurally, the Danish Central Graben has a Upper Jurassic sediment deposit section, which is one of the relatively thick sequences in the North Sea area. The thicknesses of the section is more than 4 km. The Zechstein Basin reaches the Danish Central Graben from both the northern and the southern basins. Further, halokinesis has a significant role in the structural development, and the Southern Basin has invaluable importance for oil and gas fields for the area (Møller and Rasmussen, 2003).

The growing stage of the Danish Central Graben system occurred between the Middle Jurassic and Early Cretaceous time (Figure 2.4). The combination of normal faulting and mobilization of the Zechstein and Triassic salts has impact on the growing process. Yet, the Mid North Sea Dome and uplifting erosion influenced the Danish Central Graben in the Early Jurassic and resulted in a regional unconformity on the Mid-Jurassic basement ( Møller and Rasmussen, 2003).

The rifting phase in the Danish Central Graben was addressed by more than one tectonic events from the Mid-Jurassic to Early Cretaceous followed by the collapse of the Mid North Sea Dome. The first tectonic event occurred in the Mid-Jurassic and defined by settling in a NNW-SSE to N-S trending striking fault.

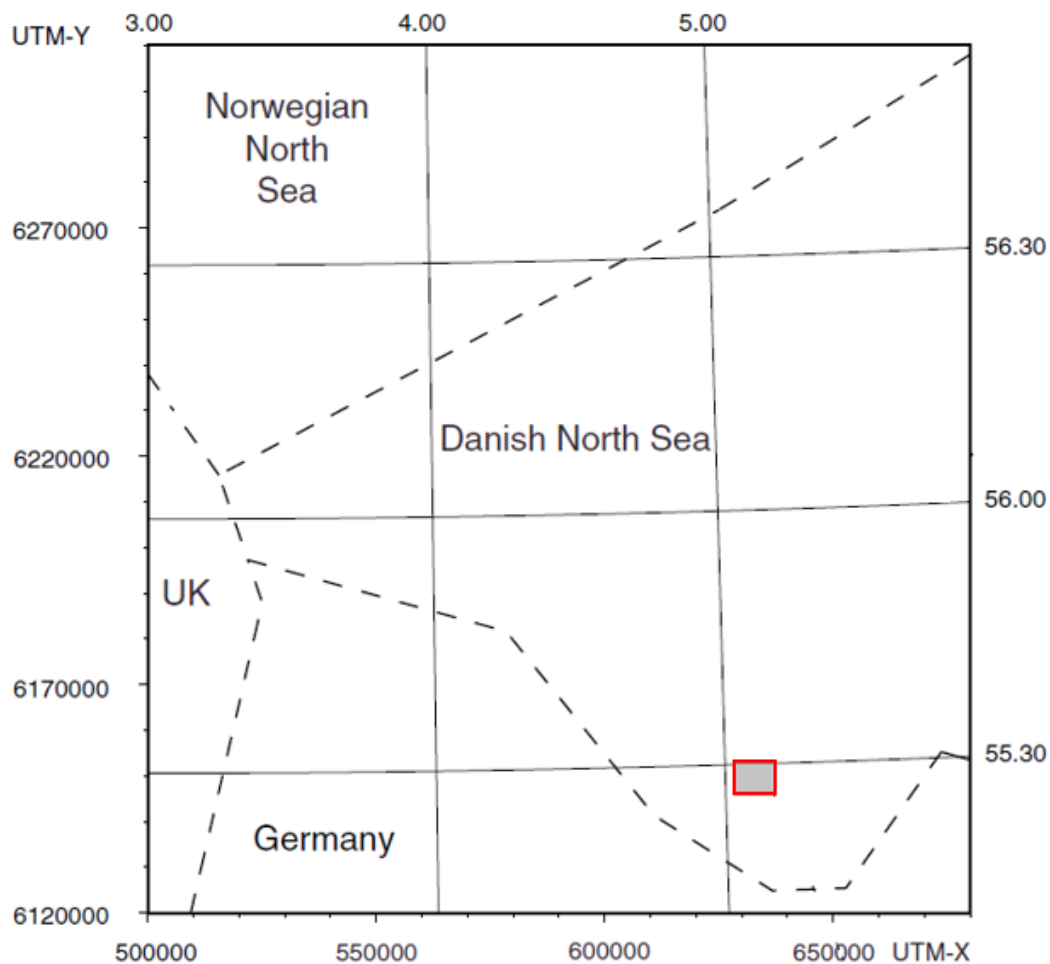


Figure 2.3. Location map of the Danish Central Graben in respect to the Danish North Sea. The study area is outlined in red (Vejbæk and Kristensen, 2000).

At this stage, salt movement took place and salt pillows were formed. The second tectonic event occurred in the Late Jurassic and thick sediments were deposited in the hanging walls of the fault system trending NNW-SSE (Figure 2.4). This deposition led to salt movement and salt bodies were formed. The last tectonic event was caused by reactivation of the NNW-SSE trending faults and resulted in minor thrusting inversion and halokinesis (Møller and Rasmussen, 2003).

In addition, the strong movement on the Cretaceous to Early Tertiary has impact throughout the Danish Central Graben. It is significant to underline that several hydrocarbon traps in the area were formed as a result of the movement (Megson, 1992).

The northern and southern part of the Danish Central Graben have limited Zechstein deposits, in the Søgne Basin and Salt Dome Province (Møller and Rasmussen, 2003). Salt formation is marked as initiated in the Triassic time under the influence of the expansion of the Triassic deposits.

## **2.5. THE SOUTHERN SALT DOME PROVINCE**

The Southern Salt Dome Province is located in the southern Danish Central Graben, extends into the Southern Zechstein basin (Figure 2.5). The province shows intrusions, diapirs, and swells in the salt structures. The Southern Salt Dome Province was formed at the time of development of Kimmeridgian/Volgian half-graben. Consequently, the Pre-Zechstein basin floor has a slightly flat structure. The Dan Transverse Zone and N-S trending faults have the primary influence during the formation process (Duffy et al., 2013). The importance of the Southern Salt Dome Province in this study is included the targeted area.

## **2.6. SALT STRUCTURES**

Although the Zechstein group salt is expanded, it is limited to the Northern and Southern Permian basins. In these areas, salt deformation was interpreted as occurring during the Triassic (Gatliff et al., 1994). However, Hodgson et al., (1992) suggest that halokinesis/salt tectonics (gravity creep) started in the Permian time (syn-Zechstein).

The Zechstein salt thicknesses vary in the Danish Central Graben. While salt thickness decreases northward, the salt thickness increases in the southern part of the graben and reaches the highest level. The Western and Northern part salt deposition are not

enough resolve seismically due to their thickness (Duffy et al., 2013). On the other hand, salt thickness increases once again around the salt structures in the Sogne Basin, which is the northern part of the graben.

The Zechstein salt is thin and welded around most salt structures (Duffy et al., 2013). The Danish Salt Dome Province represents several different salt structure styles that differ from salt diapirs, which are penetrated by their sedimentary cover to non-penetrated salt cored anticlines. Salt structures (Figure 2.5) are represented in the southern domains as pillows such as the Karaka salt pillow, as diapir such as the Skjold salt structure, and wall-and-sill complexes such as the Dan Salt Structure. While most of the salt structures formed as a consequence of flowage of Zechstein salt into them, the Dan Salt Structure is a rare exception.

Two dimensional seismic data was obtained from the Dan Salt Structure and interpreted. The upper part of the structure shows consistency with the Triassic salt, while the lower part is the Zechstein salt (Jorgensen, 1992). However, Sundsbø and Megson (1993) suggest that the upper part of the structure (intra-Triassic) consists of intrusion into the Zechstein salt along the Dan Transverse Zone. The location of the salt structures corresponds to the location and the orientations of the major faults in the Pre-Zechstein sequences (Duffy et al., 2013).

## **2.7. FAULT SYSTEM IN THE DANISH SALT DOME PROVINCE**

Coffee Soil Fault and Dan Transverse zone are considered as a two major fault system in the Danish Salt Dome Province.

**2.7.1. The Coffee Soil Fault.** The fault is located on the eastern margin of the Central Graben in the Danish part (Figure 2.5). The fault is a predominantly hard-linked fault system, which dips westward. Both the northern and southern sections, which have offset about 8 km wide sinistral jog in the fault trace, related to a regional high (Poul Plateau).

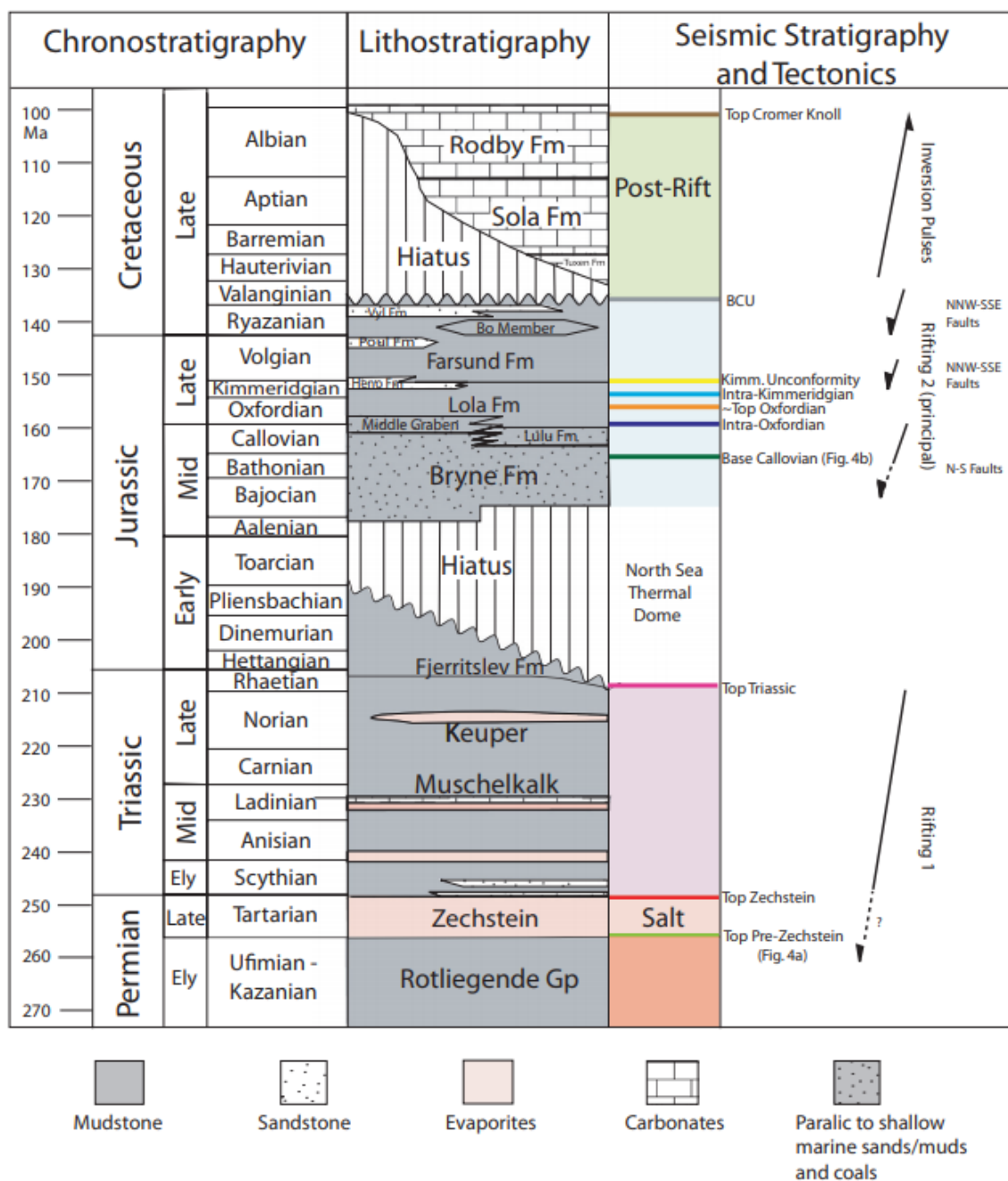


Figure 2.4. Stratigraphic framework shown ages and representative lithologies of the formations presented in the Danish Central Graben with the major tectonic events (Duffy et al., 2013).

The relationship between the Central Graben and the Coffee Soil Fault is that the strike direction of the Central Graben changes in the Danish mainland from N-S in the south to NW-SE in the north.

It represents the strike direction of the Coffee Soil Fault. In addition, the fault has different segments that vary in strike directions (Cartwright, 1987 and 1989). Moreover, it is argued that the Central Graben may be segmented by itself at the same time with the change in strike direction.

Relatively thick Triassic and Upper Jurassic sequences are placed in the area of the southern Zechtein Basin. At this location, graben is oriented in N-S direction. The Northern Zechtein Basin area, where the graben traces to Late Jurassic, had the same N-S orientation (Sundsbø and Megson, 1993).

The area of the segmented graben was oriented NW-SE. There is no considerable thickness of Triassic deposits. However, the area includes Upper Jurassic shales up to 4 km, locally. It is believed that the variation of the strike in stratigraphic thickness might be associated with variation in the slip rates. Differences in the slip rates along the fault in the separate segments have forced lateral movements on the connected basin sequences (Sundsbø and Megson, 1993).

**2.7.2. Dan Transverse Zone.** Cartwright (1987) was first to mention the Dan Transverse Zone and suggests that the origin of this transverse zone was as a Tornquist-parallel basement trend and was reactivated over the time. The Dan Transverse Zone was mapped in the WNW-ESE direction. However, the current study suggests the direction to be more NW-SE. Gorm, Skjold, and Dan salt structures were aligned above the Dan Transverse Zone striking NW-SE.



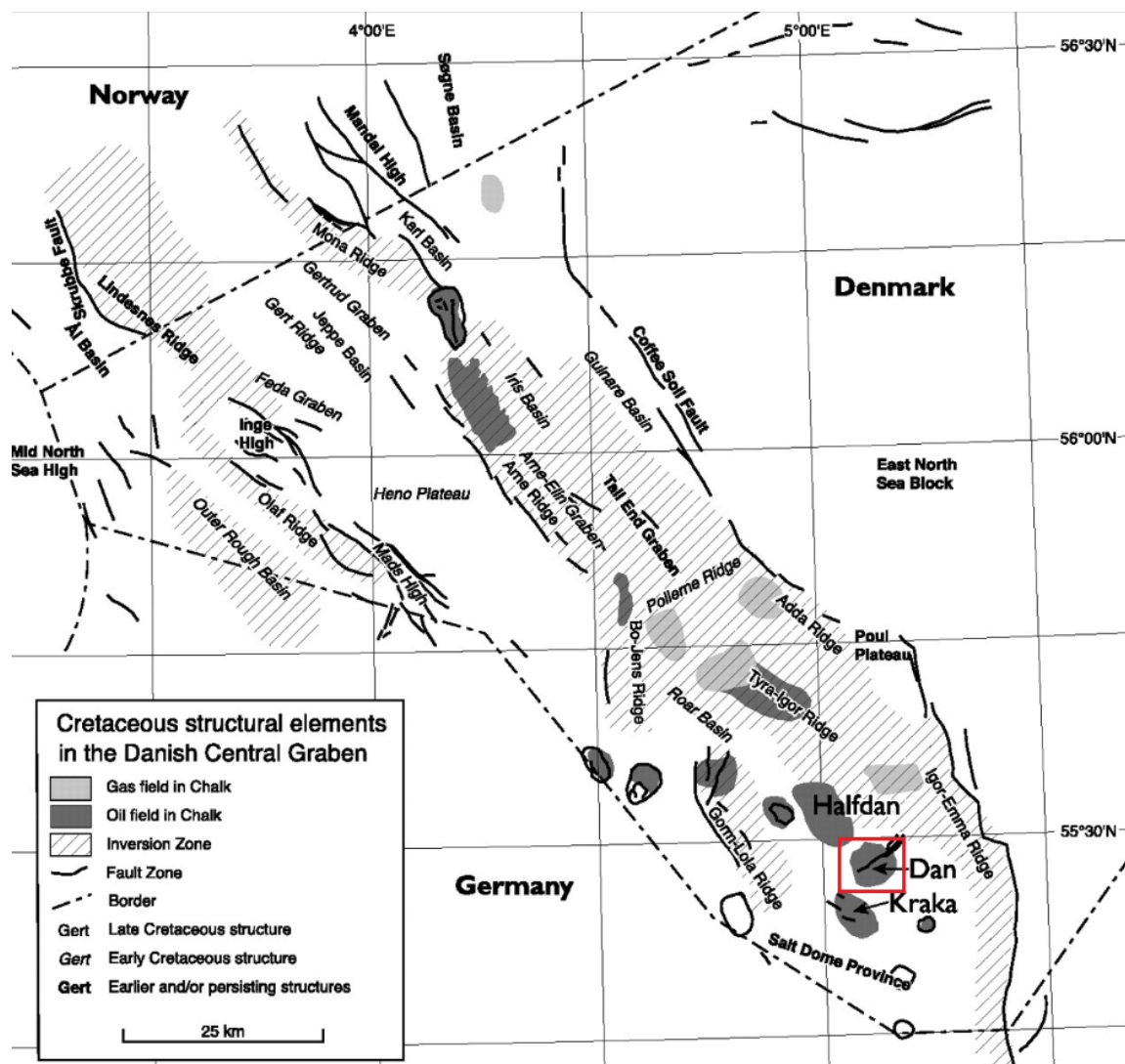


Figure 2.5. Danish Central Graben structural elements with faults at the Base Chalk level. Oil and gas fields with chalk reservoirs are also shown. The study area is outlined in red. Modified from (Klinkby et al., 2005).

## 2.8. SALT MOBILIZATION AND FAULT RELATIONSHIP

The Zechstein Salt has an impact on decoupling sub-Zechstein and supra-Zechstein, which is the cover part. Normal fault arrays in the Danish Salt Dome Province exist and were observed in both the sub-and supra- Zechstein. At the place that lacked of the salt layer, rooted basement fault in the pre-Zechstein moved upward, replacing the overburden successions and forming a thick-skinned normal fault. Pre-Zechstein faults disappeared at

the base of salt in which the Zechstein salt is thick. These faults led to the salt to deform and develop salt structures such as pillows and diapirs (Duffy et al., 2013). Characteristically, high amplitude and short wavelength fold structures form above these structures. This folding allows regional thick-skinned extension and thin-skinned faulting that might be driven by fault or load. In addition, initiated salt mobilization is cause to the development of high density fault arrays (Duffy et al., 2013) (Figure 2.6).

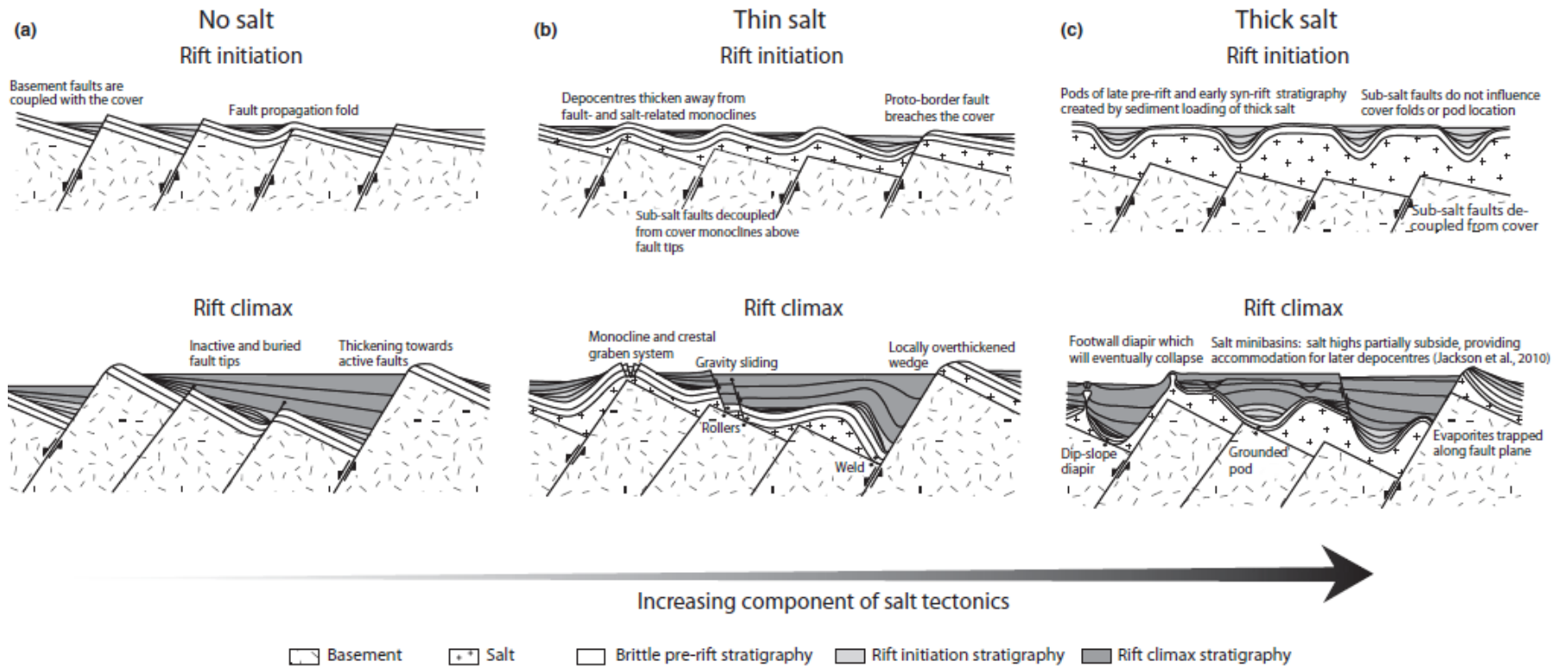


Figure 2.6. Schematic cross sections shown the influence of the ductile salt layer on the rift structural style and stratal geometry style during rifting phase (Duffy et al., 2013).

### **3. THE MARS-URSA BASIN**

#### **3.1. AREA OVERVIEW**

The Mars-Ursa minibasin is an inter slope basin on the continental slope, Northern Gulf of Mexico. It is located about 225 km south of New Orleans, Louisiana and lies in 2600-4600 feet of water (Figure 3.1).

The Mars-Ursa basin was formed by sediment accumulation during Late Miocene to Middle Pliocene time. Salt movement has been played significant role during sedimentation. Sedimentation varied over the time and the Mississippi River is the main sediment source. Sedimentation from the N-NW throughout Miocene loaded the salt and triggered evolution of minibasin formation (Bouroullec et al., 2004). The minibasin mostly composed by turbidite deposits, which are classified as lowstand deposit, and surrounded by allochthonous salt bodies (Martin et al., 2004). Further, local tectonic activity and glacia-eustacy have important role on the evolutionary stage of the area.

#### **3.2. THE GULF OF MEXICO BASIN**

The Gulf of Mexico Basin was traced to the late Middle to early Late Jurassic time (Figure 3.1). The basin was resulted in crustal extension and thinning, rifting and sea floor spreading, and thermal subsidence. There is a general agreement that the Central Atlantic and the Gulf of Mexico Basin developed at the same time that North America separated from South America and Africa (Pindel, 1985). The Gulf of Mexico Basin is a semicircular basin that is 1600 km in diameter and overfilled basin that has been supplied by sediments from North America.

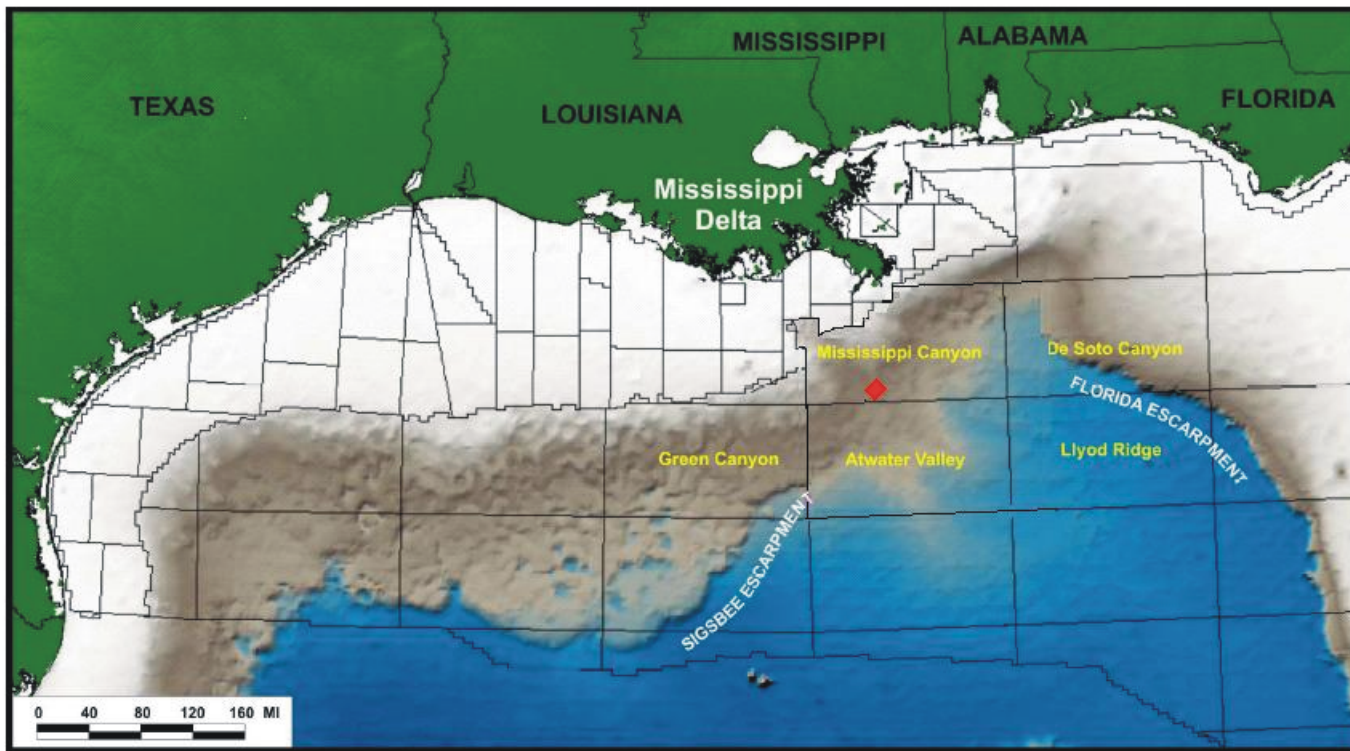


Figure 3.1. Location map of the Mississippi Canyon. The study area is outlined in red (Bouroullec et al., 2004).

### **3.3. THE MISSISSIPPI CANYON**

The Mississippi Canyon is located about 257 km southeast from New Orleans, Louisiana in the North Central Gulf of Mexico about 2000 feet below sea level. The Mississippi Canyon was formed as a part of the Mississippi submarine valley. The origin of this canyon has generally been attributed to channel entrenchment at the Mississippi River during low stand at the sea level on currents or submarine gravity flows (Coleman et al., 1982).

### **3.4. THE MARS-URSA BASIN**

The Mars Ursa Basin is a salt withdrawal minibasin and located about 225 km south of New Orleans, Louisiana in the Northern Gulf of Mexico slope and encompasses about 2600-4600 feet of water. The Mars-Ursa Basin was formed as a result of sediment accumulation from Late Miocene to Middle Pliocene time. This minibasin is mostly composed of turbidite deposits and is surrounded by allochthonous salt bodies (Martin et al., 2004). The Mars-Ursa Basin is an important part of the tabular salt minibasin province. The greater part of the continental slope is bounded by this province, which is a part of a Neogene counter-regional salt system. Salt diapir collapse occurred because of the gravity spreading or regional extension, led to initiation of the minibasin formation during the Miocene sedimentation from N-NW stored (Bouroullec et al., 2004).

### **3.5. MINIBASINS**

Minibasins are a type of basin generally associated with a mobile salt environment and characteristically form in a sub-circular shape a few tens of kilometers in diameter. Minibasins are related to the interaction between the Cenozoic growth faulting and salt mobility in the Northern Gulf of Mexico Basin (Worrall and Snelson, 1989).

The term "minibasin" is redefined as a syn-kinematic basin subsiding into a proportionally thick allochthonous or autochthonous salt. While minibasins downdip margins bounded by a counter regional faulting, both the updip margins and sides are restricted by growth faults or salt domes and salt ridges, occasionally with the strike-slip dip. In many cases, the loading of the thick sedimentary filling causes density inversion on the minibasin formations (Jackson and Talbot, 1991). However, a density driven mechanism might not be the only reason to cause minibasins to subside (Hudec et al., 2009).

### **3.6. SALT STRUCTURE**

The tectonic evolution of the Gulf of Mexico began as a consequence of inter-continental rifting between North America and the Yucatan Block in the Middle Jurassic (Salvador, 1991). The flooding of the seawater occurred discontinuously and repeatedly into the low-lying rifted area throughout the Late Callovian to Early Oxfordian time. This sea water flooding resulted in extensive salt deposition known as Louann salt (Salvador, 1991).

Deposition of the salt in the rift basin took place before the seafloor spreading. This depositional process remained till the Kimmeridgian (Bird et al., 2005). With restricted marine conditions, an increasingly large body of the water with normal salinity was replaced with the shallow hypersaline water bodies. As a result, the Callovian salt sequence was produced (Salvador, 1987).

The continental rifting in the basin produced about 70 m.y. and resulted in an a counterclockwise rotation of the Yucatan Block. This rotation started on the Late Callovian to Early Oxfordian. The counterclockwise rotation of the Yucatan Peninsula Block away from the northern part of the Gulf of Mexico led to the opening of the basin. The rotation and southward movement of the Yucatan Block gave rise to regional extension.

This regional extension initiated the passive margin state of the basin margins along with the formation of a central band of crust formed during the Kimmeridgian (Salvador, 1991). As a consequence of the rifting process, the Louann salt deposit was divided into two parts, which are presently located in the US part of the Northern Gulf and in the Mexican part of the Southern Gulf (Buffer and Thomas, 1994) (Figure 3.2).

### **3.7. SALT MOBILIZATION AND FAULT RELATIONSHIP**

The Gulf of Mexico Basin region contains various structural features that have mostly been created by gravity acting on an unstable substrate in a nonorogenic environment. The salt tectonics, growth fault, and listric fault known as, normal growth faults, associated with rollovers are interacting with each other. This interaction creates a wide variety of features (Nelson, 1991). Growth fault systems are common structures of extensional systems resulting from gravity gliding above salt. During the stable tectonic conditions of the Cretaceous and Cenozoic time, sediment loading stimulated the movement of the Louann salt and the development of growth fault system (Konyukhov, 2008). Faulting in the minibasin is generally associated with salt diapirism (Worall and Snelson, 1989). In the study area, active and reactive diapirism have been observed. These diapirisms are accompanied by normal faults and located along the updip edge of a salt sheet.



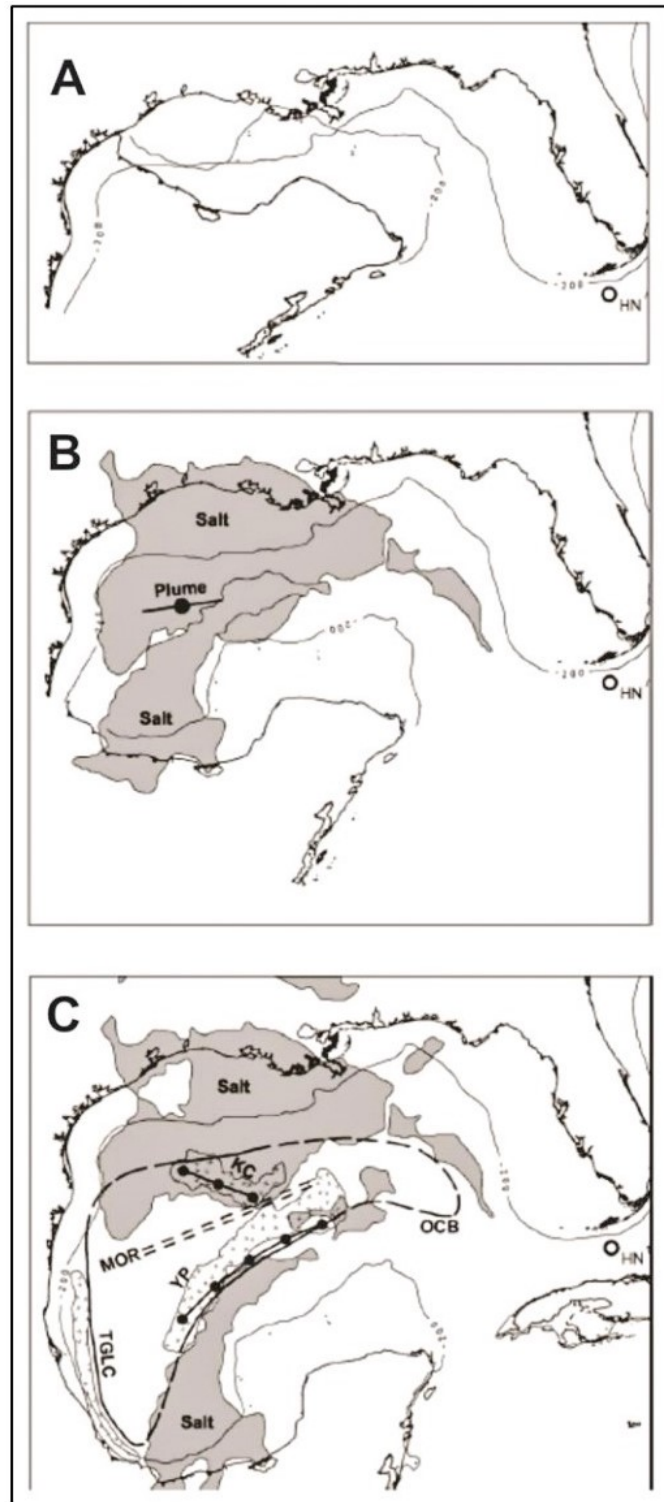


Figure 3.2. Diagram shown Deposition of the salt. A.) Initial Jurassic pre-rift position of Yucatan Peninsula; B.) Jurassic rotation, continental crust extension and seafloor spreading; C.) Rotation and present position achieved (Bird et al., 2005).

## 4. SALT TECTONICS

### 4.1. INTRODUCTION OF SALT

Salt is an evaporitic rock that is composed mostly of halite. However, salt bodies may contain a variety of other evaporitic minerals, such as evaporitic carbonates, anhydrite or its hydrated form, gypsum, and also non-evaporitic rocks that might be accumulated during salt movement (Hudec and Jackson, 2007). Evaporates are usually settled when surface and near surface brine becomes saturated as a consequence of solar evaporation (Warren, 1999).

In general, deposition of evaporates may be present in four settings. These are cratonic basins, syn-rift basins, post-rift passive margins, continental collision zones, and foreland basins. Approximately 120 of the worlds evaporate basins have been influenced by salt tectonics. Salt tectonics may form regional extension and shortening or halokinesis, which is driven by gravity (Hudec and Jackson, 2007).

Salt has its own deformation style and occurs on a regional scale and creates different shapes and sized salt structures such as linear and point source. Salt structures that are connected to point sources, rise from salt pillows at early stages to reactivated salt sheets at more mature stages (Hudec and Jackson, 2007) (Figure 4.1). For example, elongated salt structures, which rise from a line source, develop from the salt rollers to salt-wall canopies because of the increase in maturity. Reactivation of subsalt faults and folding processes during contractional regimes helps to create these types of structures (Fossen, 2010).

While salt basins and non-salt basins show some deformational style similarities, their differences are also important. Salt exhibits viscoelastic and rheologically weak character under geologic conditions. Relatively high speed of relaxation generally causes it to behave as purely viscous and, thus, flows like fluid. Consequently, under geologic

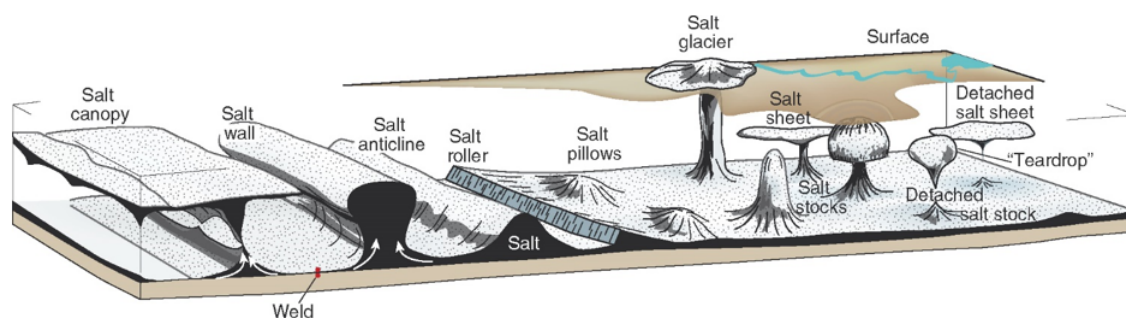


Figure 4.1. Schematic shapes of salt structures (Fossen, 2010).

conditions, salt is weaker than surrounding rocks and more favorable to deform (Hudec and Jackson, 2007). In addition, like fluid, salt is difficult to fracture, and hence faults use salt bodies as decollement surfaces, rather than shearing through the features. The physical attributes of salt are the main purpose to understand how salt deforms and how this causes deformation in the surrounding rocks.

Salt is incompressible and has an approximately density of  $2200 \text{ kg/m}^3$ , which is less than compacted sedimentary rocks, while surrounding sediments are compacted and denser than salt. Usually, salt is more buoyant than the surrounding rocks after a typical burial depth of 3000 m, and as shallow as 1600 m, when the overburden rocks begin to have larger density than rock salt (Hudec and Jackson, 2007). As a result, the density differences between the mother salt layer and overlying sediments along with buoyant properties of salt buried to a particular depth result in salt flow toward the surface by the reason of gravitationally instability (Fossen, 2010). This makes salt inherently unstable, which results in the salt basin deforming more easily than other basins. There are four main mechanisms that cause salt movement. These are gravitational, differential, displacement, and thermal loading (Fossen, 2010). Besides, heterogeneity in temperature, viscosity and lateral changes in thicknesses between the salt and the overlying sediments have a major impact on halokinetic movement (Allen and Allen, 2003). Moreover, salt has high thermal conductivity. This characteristic feature of the salt makes it important for the oil industry.

To behave as heat pipes for conduction may cause decrease in their temperature and increase in the overlying one; therefore, it can shift the gas vertically and oil windows in sediment flanks (Fossen, 2010). The velocity of the salt is more than twice higher than the velocity of the surrounding rocks. It is about 4400 m/sec (Farmer et al., 1996). As a consequence of this difference, salt structures are shown in irregularly shaped interface in seismic imaging. Salt parameters are shown in Table 4.1.

Table 4.1. Summarized information of salt properties.

|  |   |
|--|---|
| Low density: 2200 kg/m <sup>3</sup>    | High thermal conductivity                     |
| High seismic wave velocity: 4400 m/sec | Almost incompressible                         |
| Youngs modulus (E): 40 Gpa             | Impermeable                                   |
| Poisson ratio: 0.39                    | Behaving as a decollement                     |
| Viscous                                | Influence regional deformation                |
| Mechanically weak                      | Generating structural and stratigraphic traps |

## 4.2. DIAPIRISM

Salt diapirs form in four different ways: 1) reactivation piercement in between fault blocks that is related to overburden extension, 2) active piercement of salt by lifting, rotating, and shouldering aside the overburden rocks, 3) erosional piercement of salt after the removal of the overburden by erosion, and 4) emplacement of salt in the hanging wall of thrust faults (Hudec and Jackson, 2007) (Figure 4.2 ).

All these processes can take place at different times during the growth of a solitary salt structure (Hudec and Jackson, 2007). Further, salt diapirs might occasionally form by ductile thinning of the roof overburden, and at the place where salt is uncovered at the surfaces, it could rise continuously with respect to the surrounding strata in a process known as passive diapirism. The majority of the tall salt domes and walls around the world develop as passive diapirs. Most salt diapir provinces were started throughout phases of regional extension, as shown by salt bodies having a more profound portion of their flanks commonly being abutted by swarms of normal faults (Hudec and Jackson, 2007).

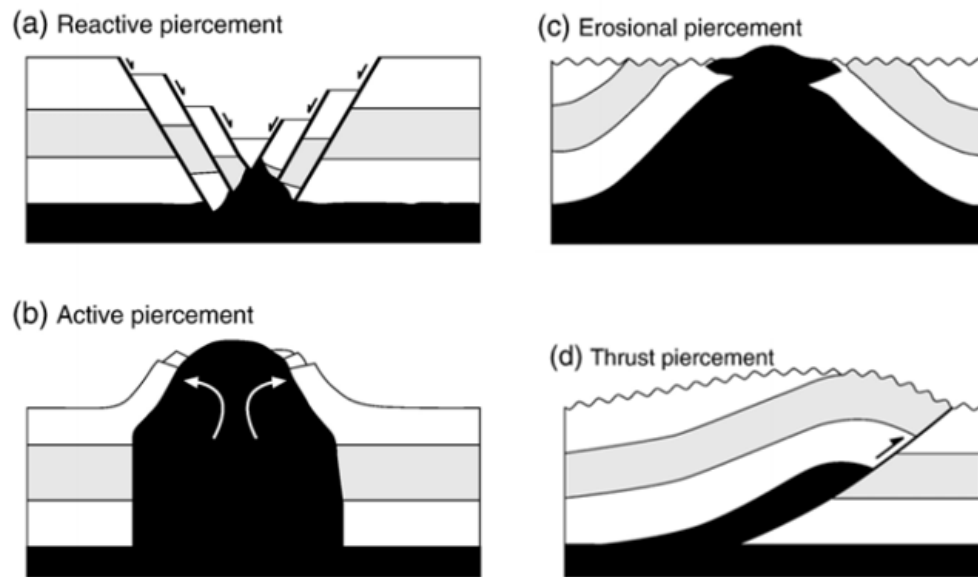


Figure 4.2. Models of diapir piercement in schematic cross sections (Hudec and Jackson, 2007).

Regional extension could result in reactivate, active, and passive diapirism in spite of the fact that salt does not fundamentally advance through all these stages. Active diapirism is controlled by gravitational forces and might proceed indeed in the event that regional extension stops. This stage occurs often and is not followed by passive diapirism as the salt proceeds to rise to the surface.

In the process of either regional compression or regional shortening, the weaker salt layers deform more easily than the surrounding rocks, usually causing the overburden to buckle. Salt might at that point stream under the buckled overburden and amplify any existing anticlinal structures. While a pre-existing salt structure undergoes shortening, a teardrop diapir might be formed, creating a steep salt weld in the former waist of an hourglass shaped diapir. Where feeder welds are greatly inclined, maintained shortening of the diapir can reactivate the welds as a thrust fault.

### 4.3. ALLOCHTHONOUS SALT

Allochthonous salt is defined as a sheet-like body of mobilized evaporate or a layered evaporate sequence that overlies stratigraphically younger rocks (Hudec and Jackson, 2007). Allochthonous salt might be based on a single salt feeder and then deposited throughout lateral spreading as an individual salt sheet or salt tongue, which might come together with other salt sheets and create canopies and nappes in a wide variety of depositional settings ranging from deepwater to subaerial.

Thirty five of the worldwide basins have been determined as salt basins containing allochthonous evaporites. Four mechanisms are suggested to understand the settlement and spreading of the allochthonous salt, which are: 1) extrusive, 2) open-toed, 3) thrust, and 4) salt wing intrusion (Hudec and Jackson, 2007).

The term "salt roller" also needs to be defined. A salt roller is a low amplitude asymmetrical structure where one side of the salt body is bounded by normal fault (Park, 1997). The presence of salt rollers indicates regional extension, which is thin-skinned perpendicular to the strike of the salt rollers.

A salt weld is a surface that separates two strata that were once separated by a salt layer and are still in contact (Rowan et al., 1999). There are two main processes that are known to produce welds: viscous flow and dissolution. It is important to note that welds in autochthonous and allochthonous salt might be formed in major structures in an evaporate basin where petroleum and mineral discovery may hinge on whether salt welds act as seals or windows for migrating hydrocarbons or dissolved metals.

When the salt is exposed to meteoric water, it dissolves easily (e.g., Johnson, 1981). Salt dissolution can also create accommodation space and influence sediment routing systems, which can be independent of tectonic and sea level effects (e.g., Gutierrez, 2004). All these salt features can be found in salt basins that have undergone tectonic extension and compression, including the Central North Sea Basin and the Mars-Ursa Basin of Gulf of Mexico.

## 5. DATA AND METHODOLOGY

### 5.1. SEISMIC DATA

The Dan Field data set is a grid of 3D time migrated seismic reflection data covering an area of  $129.4 \text{ km}^2$ . The survey has 804 inlines and 997 crosslines and the spacing is  $12.5 \times 12.5 \text{ m}$  (Figure 5.1). The survey has a sampling interval of 0.004 second and covers a two way travel time (TWT) of 5 second. The study area contains M1 and M8, namely two well data. The data set was provided by the Geological Survey of Denmark and Greenland (GEUS) for this study.

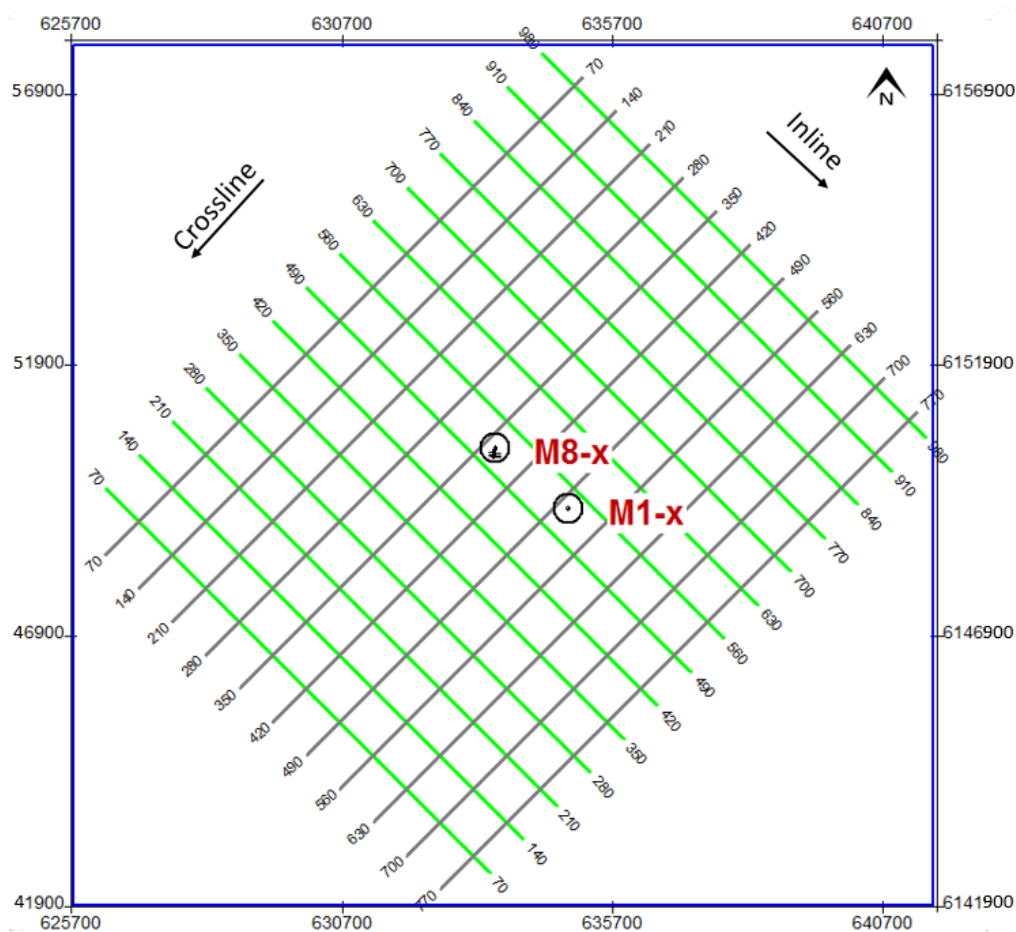


Figure 5.1. Base map of the Dan Field.

The Mars-Ursa Field data set is a grid of 3D time migrated seismic reflection data set includes 28 Mississippi Canyon (MC) blocks on the western flank of the MC in the North Central Gulf of Mexico. The survey has 723 inlines (between 4366 and 5088) and 1266 crosslines (between 645 and 5088) with spacing 87.5x87.5 m (Figure 5.2). The survey has a sampling interval of 0.004 second and covers a two way travel time (TWT) of 10 second. G3D1312-001 3D, namely Mars-Ursa basin data set was provided by the Bureau of Ocean Energy Management for public study.

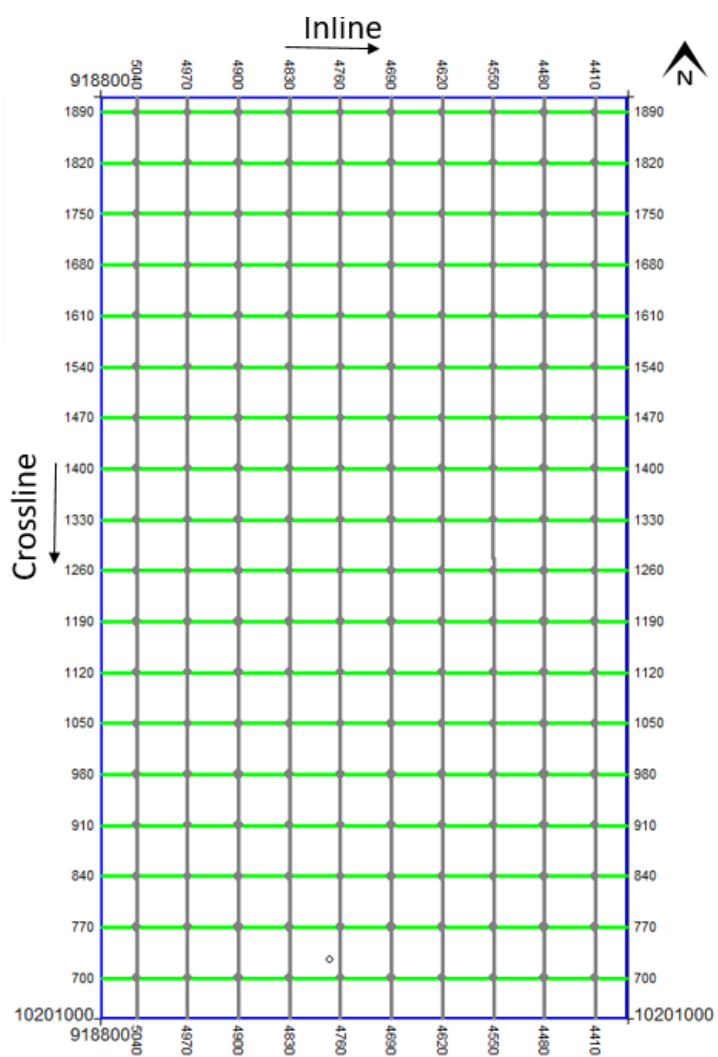


Figure 5.2. Base map of the Mars-Ursa Field.



## **5.2. METHODOLOGY**

The Kingdom software is used for geophysical and geological interpretation. The VuPak module is performed to display horizons, faults, and salt structures in a 3D cube. The Petrel software is utilized to generate seismic attributes, which are Variance and RMS amplitude.

The following steps were organized for seismic interpretation in this study,

1. Seismic data, well locations, and well logs information were checked after they imported to the both Kingdom and Petrel software.
2. Seismic interpretation of key horizons, faults, and salt were performed.
3. Structure maps for the interpreted surfaces were generated.
4. Seismic attributes were also generated and used to complement the seismic interpretation.

## 6. SEISMIC ATTRIBUTES

Seismic attribute analysis uses variations in the amplitudes and tracks these features through the entire data volume. This approach can generally enhance the imaging of geologic features such as faults, fractures, and specific stratigraphic features (Weimer and Davis, 1996).

The Petrel software was used to compute seismic attributes, and the data were imported back to the Kingdom software for interpret. Computing different types of seismic attributes helps to interpret structural elements and discontinuities such as faults and salt bodies.

### 6.1. VARIANCE

The main working principle of the variance attribute is to measure horizontal continuity in amplitude (Van Bemmelen and Pepper, 2000). The variance attribute is a powerful tool for determining salt bodies, based on the difference from broken reflectors (salt) to continuous reflectors (minibasins), faults, and channel edges on both horizon slice and vertical seismic profile.

In the time slice at 2.012 s from the Dan Field (Figure 6.1), visibility of majority faults are limited and the channel system is not detectable. However, in the variance time slice, faults, fractures, and channel system are visible (Figure 6.2 and 6.3).

In the time slice at 2.066 s from the Mars-Ursa basin (Figure 6.4), visibility of majority faults, fractures, salt bodies, and minibasins are limited. However, in the variance time slice, faults, fractures, salt bodies, and minibasins are visible (Figure 6.5).

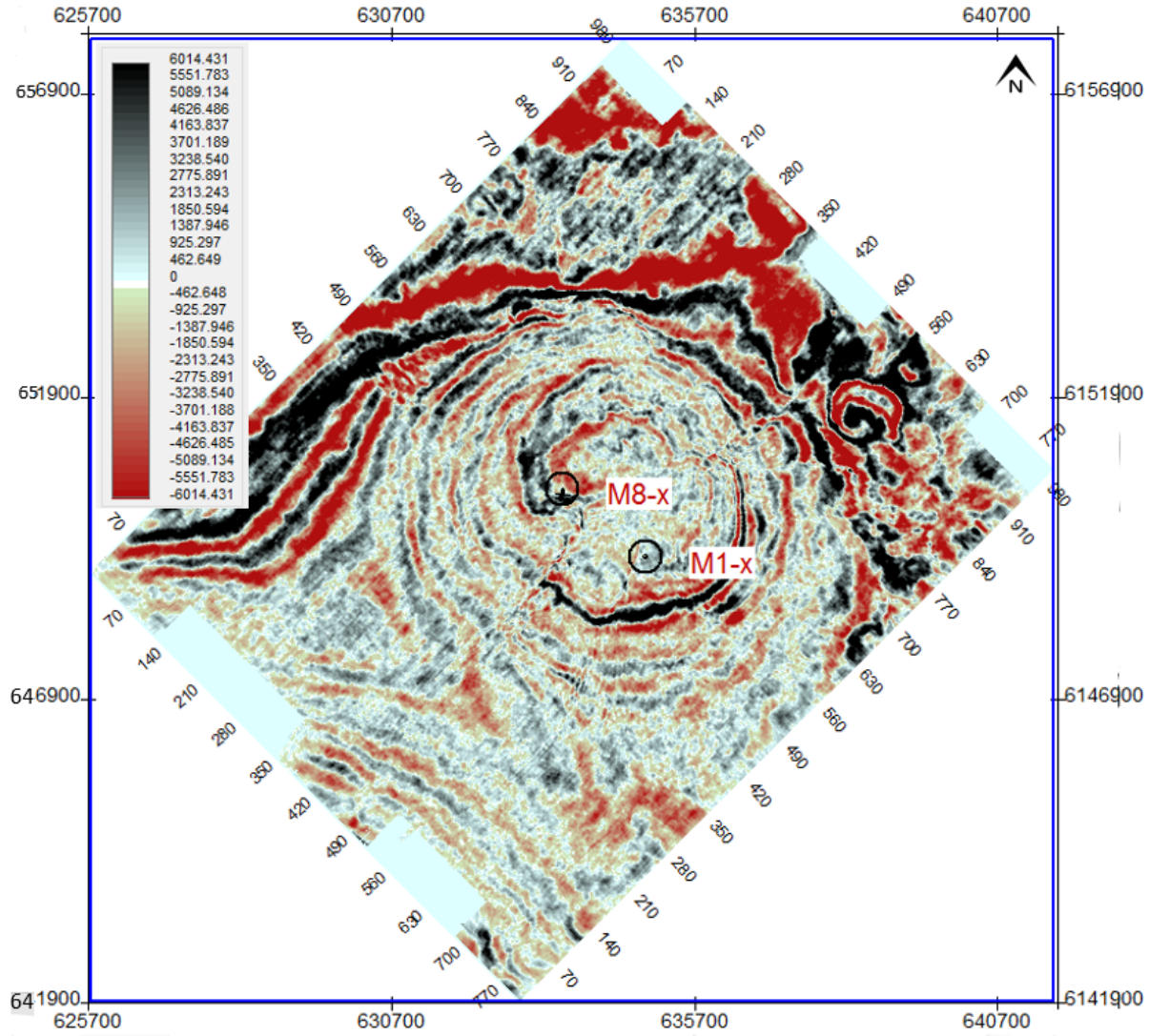


Figure 6.1. Time slice at 2.012 s from the Dan Field. Faults and channel system are invisible.

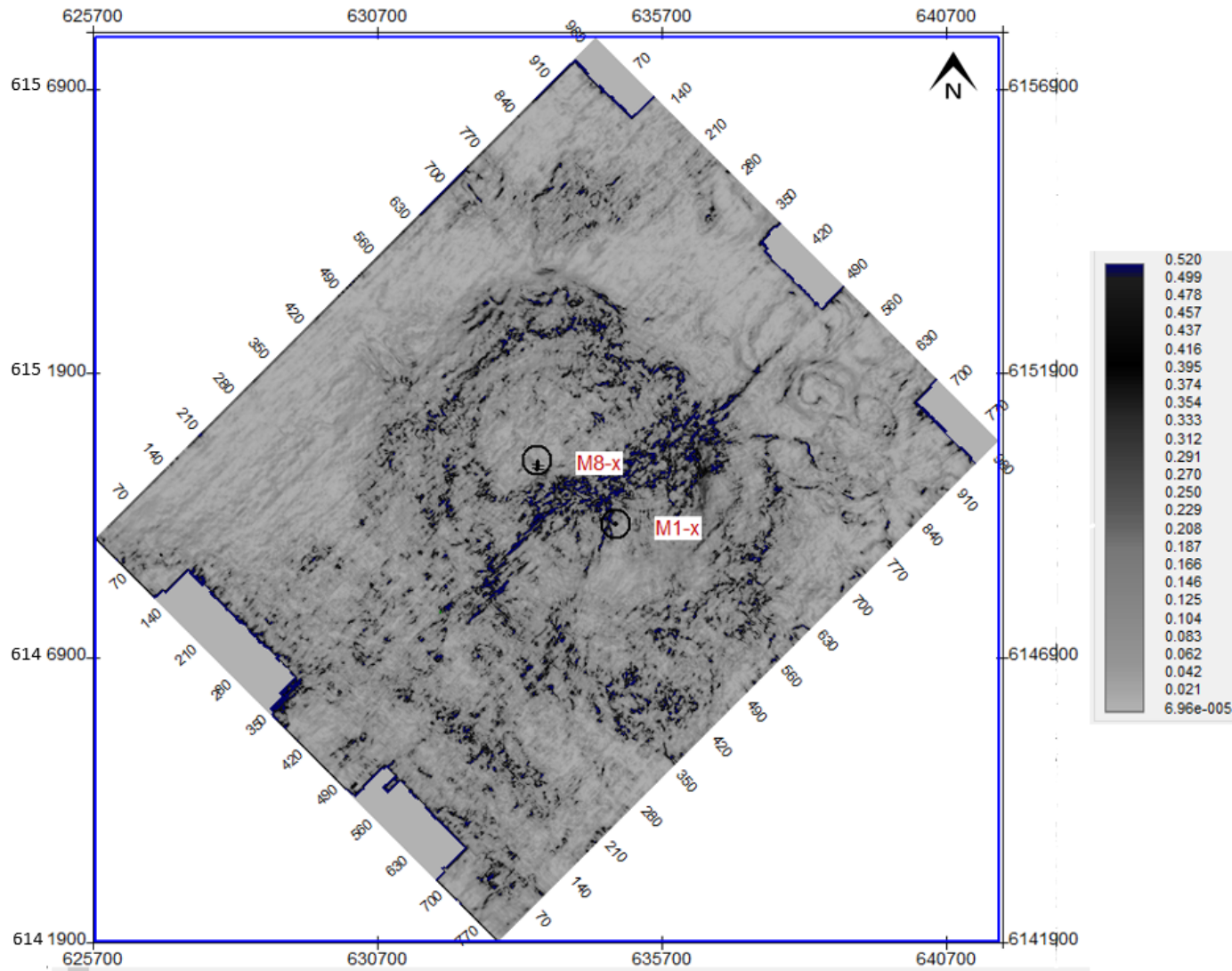


Figure 6.2. Variance attribute time slice at 2.012 s from the Dan Field shown uninterpreted faults and channel system.

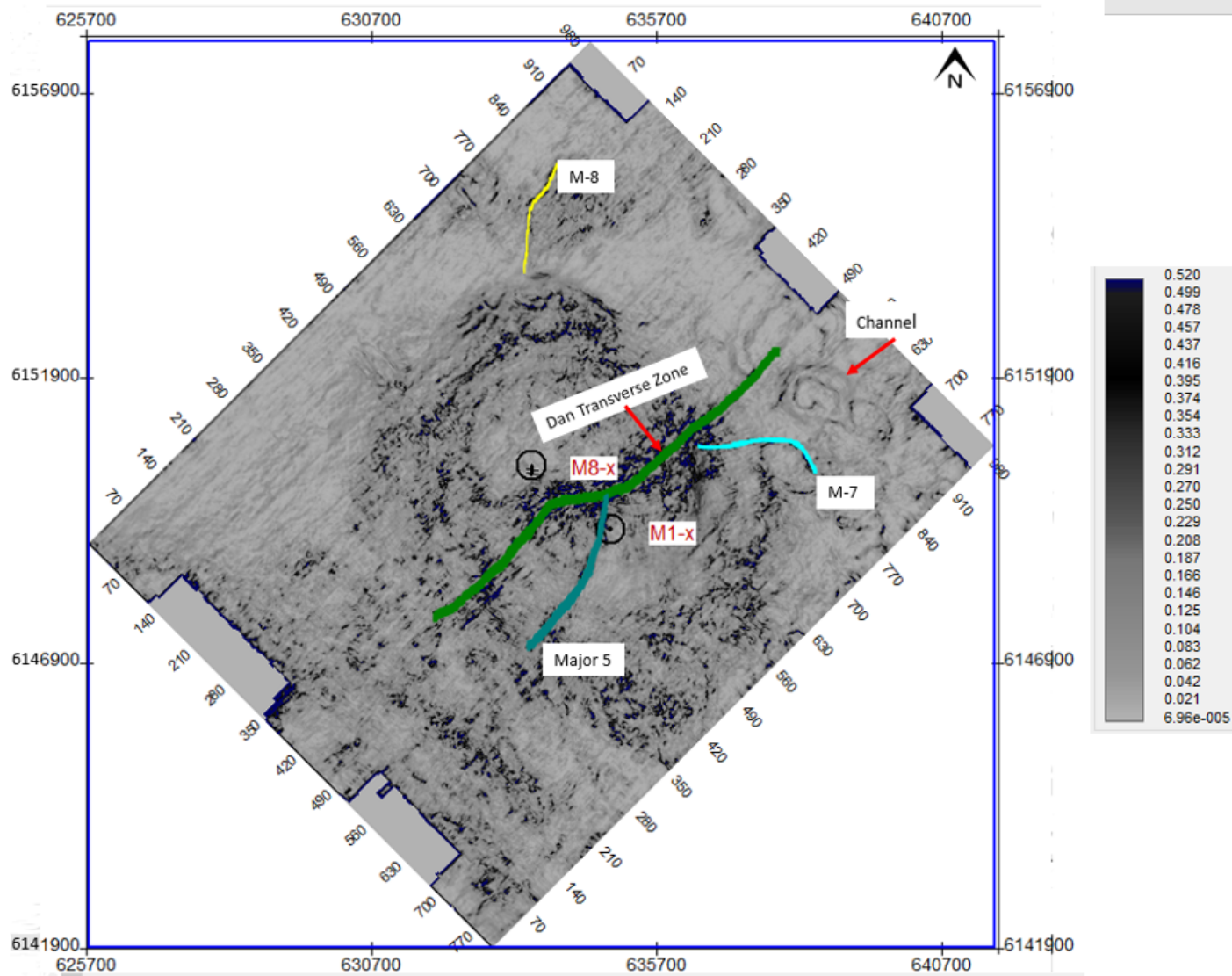


Figure 6.3. Variance attribute time slice at 2.012 s from the Dan Filed shown interpreted faults and channel system. Faults and channel system visibility is significantly improved.

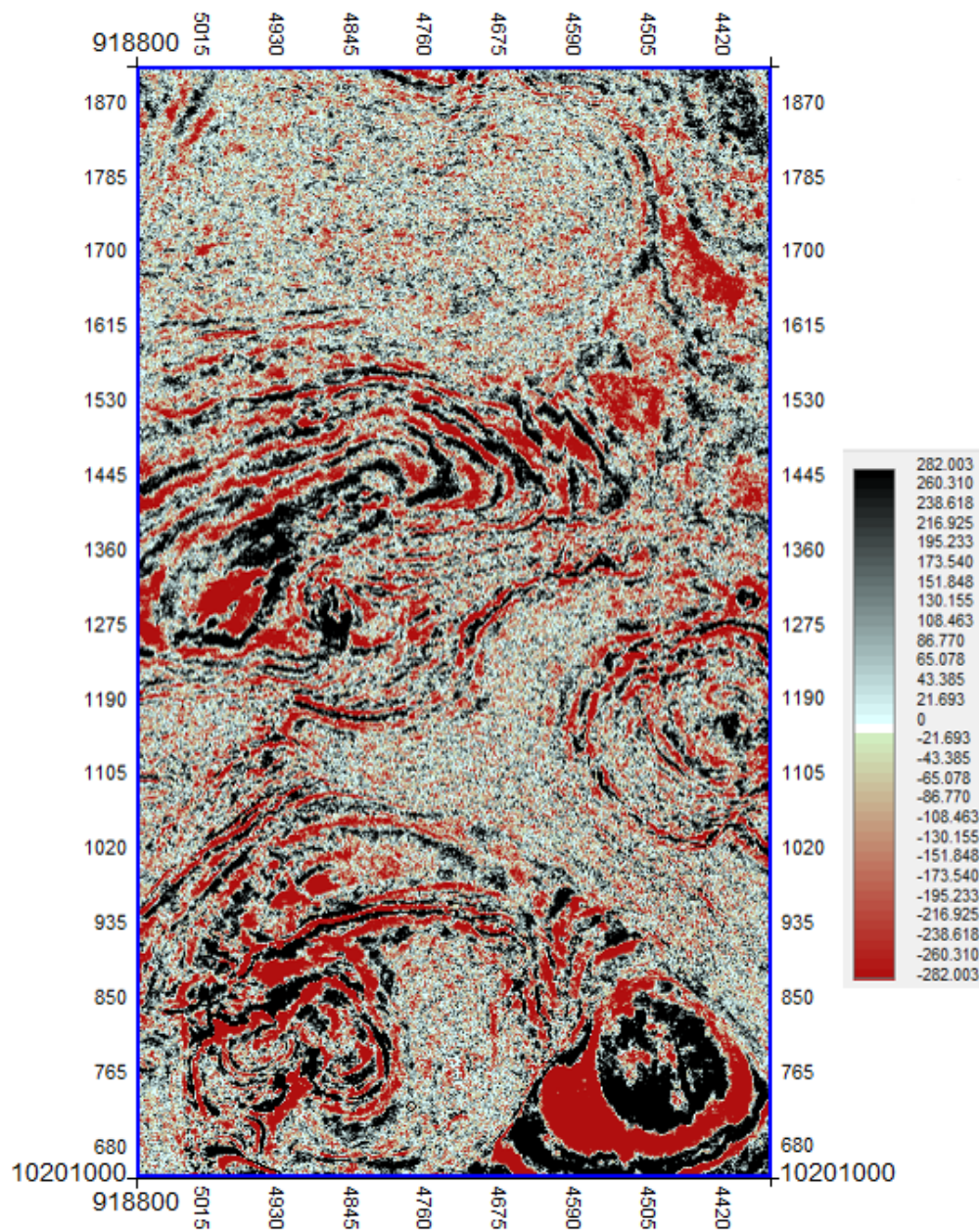


Figure 6.4. Time slice at 2.066 s from the Mars-Ursa Basin. Salt structures and minibasins are invisible.

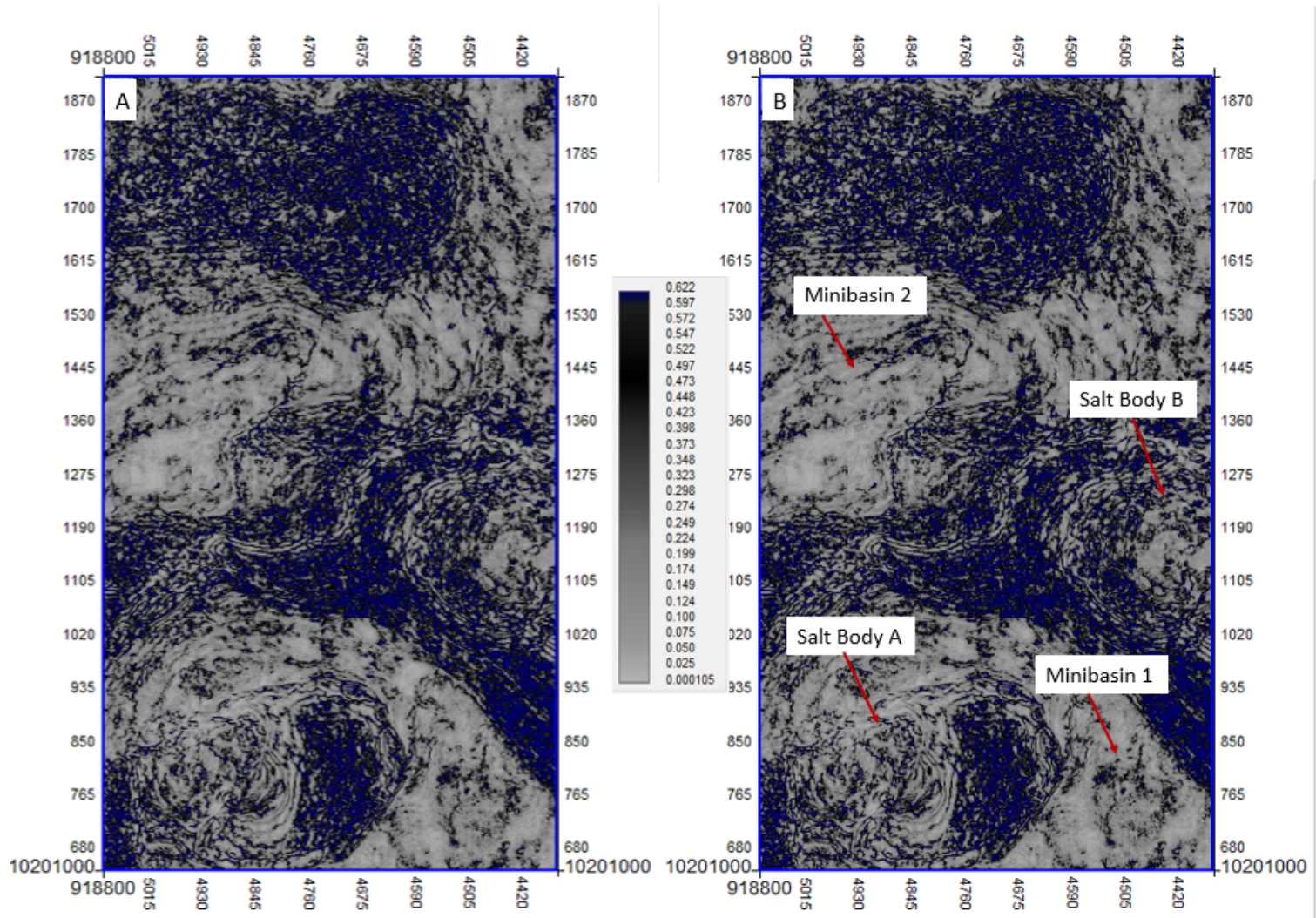


Figure 6.5. Variance attribute time slices. A.) Variance attribute time slice at 2.066 s from the Mars-Ursa Basin. Salt structures and minibasins visibility is significantly improved. B.) Variance attribute time slice at 2.066 s shown interpreted salt structures and minibasins.

## 6.2. RMS AMPLITUDE

Root Mean Square (RMS) is the amplitude computed from the sum of the squared amplitude divided by the number of samples in a specified time window. This produces as measure reflectivity and as a direct hydrocarbon indicator within a zone of interest (Chopra and Marfurt, 2008). The RMS amplitude emphasizes the variation in the acoustic impedance in a selected time window. Generally, the high acoustic impedance variation represents high values of RMS. The RMS attribute is used to identify gas chimney and other direct hydrocarbon indicators such as bright spot.

The gas beneath the seafloor is related to a buried petroleum system in the Mars-Ursa Basin. Overlying sediments led to an increase in pressure and the salt body moved upward. The upward movement of the salt continued and caused salt deformation, fracturing, and faulting within overlying sediments. Fracturing and faulting assist hydrocarbon in migrating from the subsurface to the seafloor. Free gas within sediments causes a decrease in seismic velocity and density and an increase in acoustic impedance between hydrate bearing sediments and free gas bearing sediments (Satyavani et al., 2008). Salt Body A shows gas hydrate, gas chimney, and bright spots in RMS windows (Figure 6.6 and 6.7).



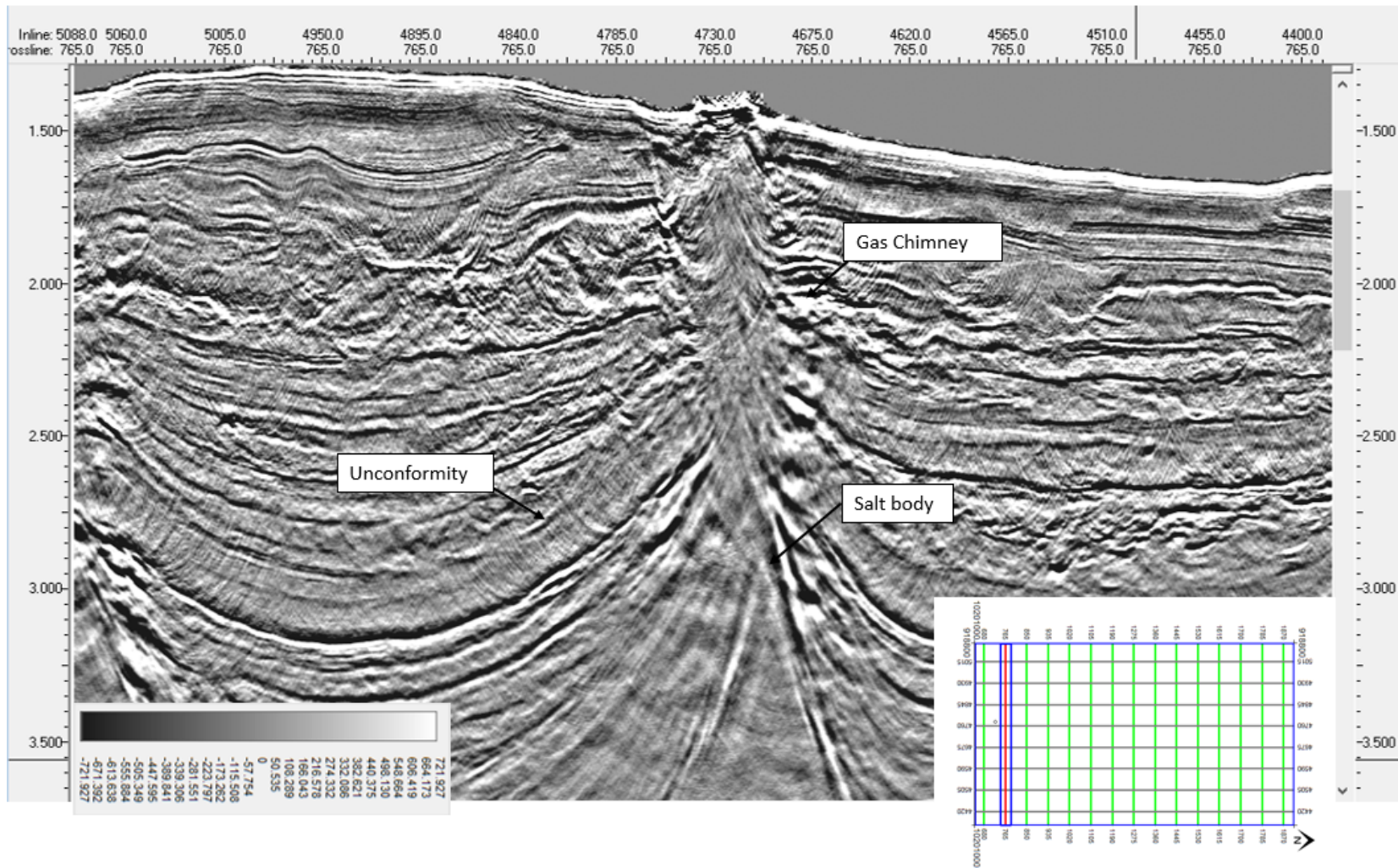


Figure 6.6. Vertical seismic section of Crossline 765 shown with gas chimney, salt body, and unconformity.

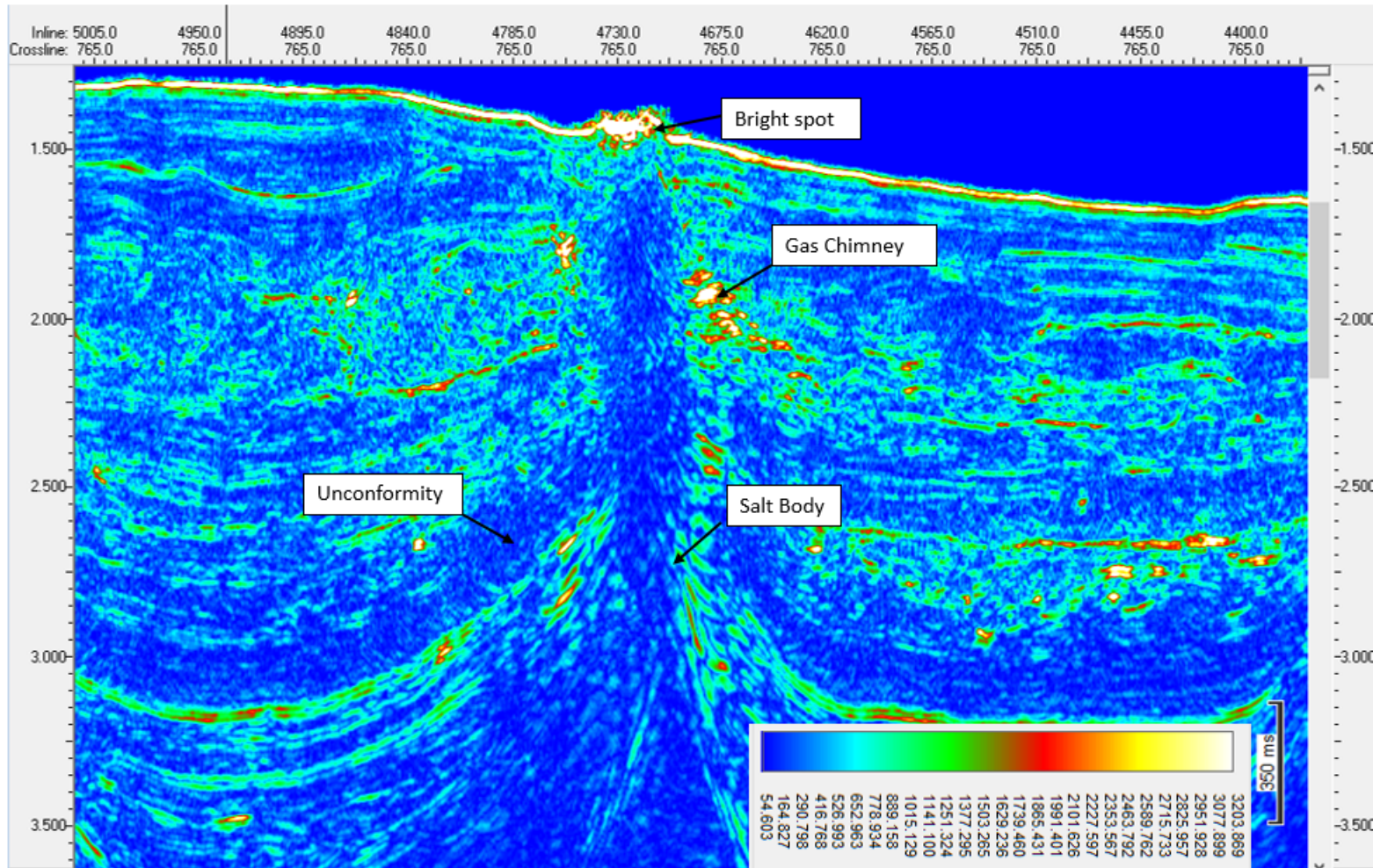


Figure 6.7. RMS amplitude attribute window shows bright spots, gas chimney, salt body, and unconformity in Crossline 765 from the Mars-Ursa Field. Shallow high amplitude events related to the presence of gas and different packages of lithologies are easily identified in RMS amplitude attribute window.

## **7. SEISMIC INTERPRETATION**

Structural interpretation is the primary tool for understanding fundamentals of subsurface geometries and their patterns. Structural interpretation is performed for faults, horizons, and salt to gain knowledge of structural features of the Dan Salt Structure and the Mars-Ursa Basin.

### **7.1. FAULT INTERPRETATION**

Faults are generally indicated by observation of discontinuities or breaks in reflections. Abrupt vertical displacement of several reflectors along a distinct line such as a fault plane, is the best indicator for the presence of faults (Marillier, 2006). Identifying interaction between salt and faulting is a key factor to understand what type of salt movement took place during the deformation process. Major and minor faults are observed and interpreted in both areas (Figure 7.1).

Dan Transverse Zone is a major fault in the Dan Structure, in the southern salt dome province. Orogeny on the Caledonian time caused the reactivation of the basement fault. This reactivation led to the development of the Dan Transverse Zone, which has affected much more of the halokinetic movement in the southern salt dome province (Sundsbø and Gowers, 1993). During the Late Proterozoic to Early Paleozoic times, the Dan Transverse Zone acted as an extensional plate margin (Evans et al., 2003). The Dan Transverse Zone was interpreted as a NW to SE trending normal fault (Figure 7.1 and 7.2).

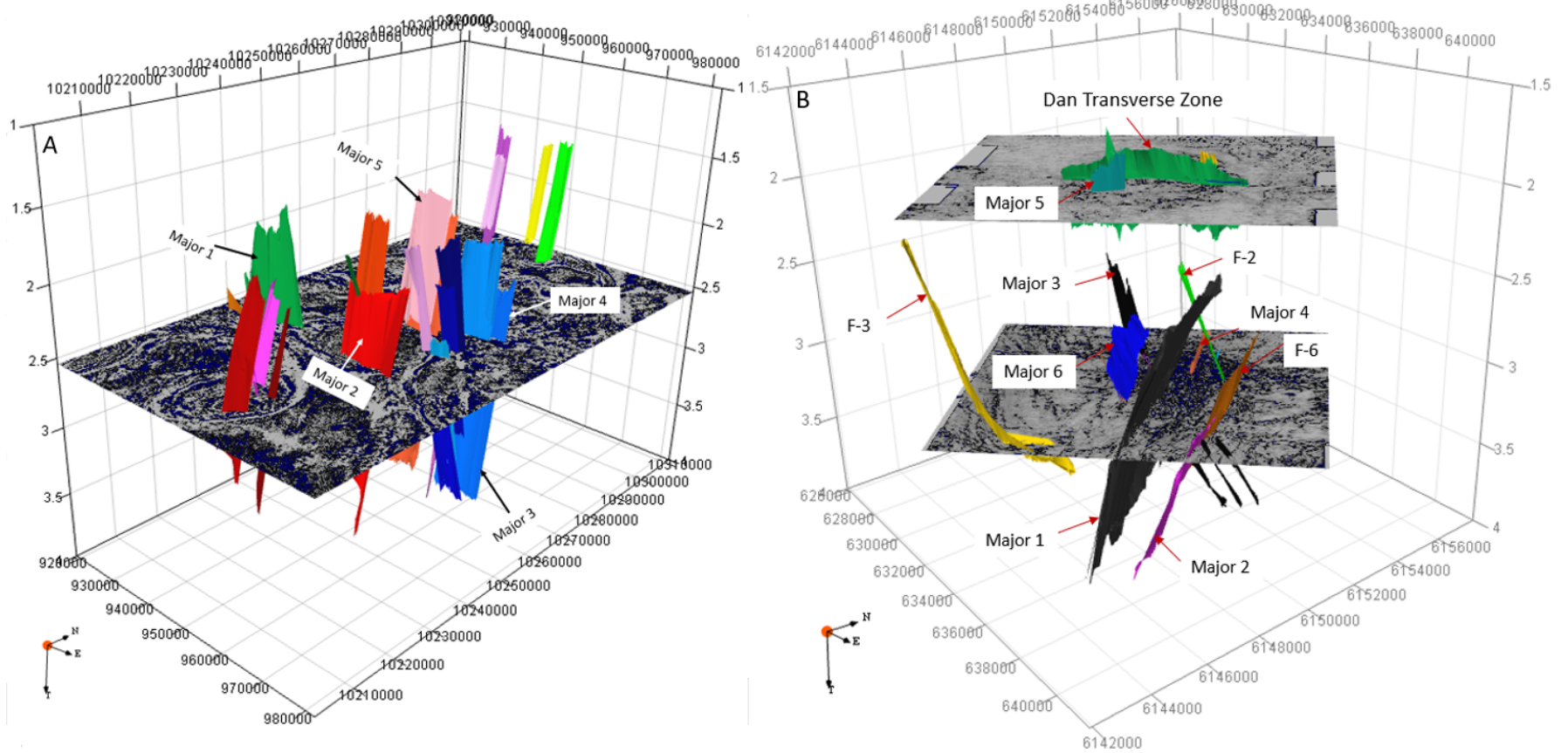


Figure 7.1. Three-dimensional visualization of interpreted major and minor faults. A.) Three-dimensional visualization of interpreted faults in Mars-Ursa Filed. B.) Three-dimensional visualization of interpreted faults in Dan Filed.

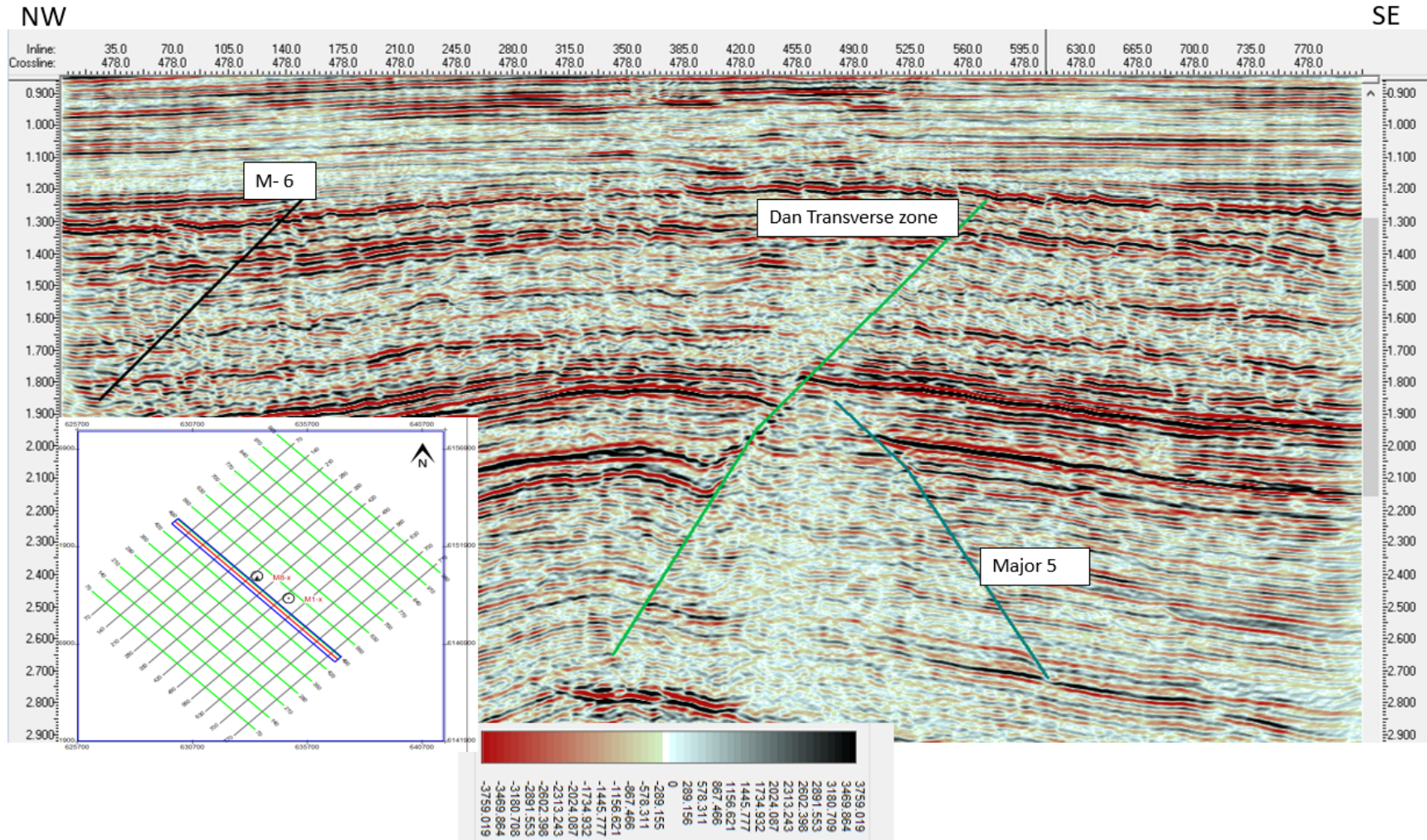


Figure 7.2. Vertical seismic section of Crossline 478 shown with interpreted faults. Green fault represents NW-SE trending Dan Transverse Zone.

## **7.2. SALT INTERPRETATION**

The salt has more than twice higher velocity than the velocity of the surrounding rocks. Consequently, in seismic imaging, salt structures are shown in an irregularly shaped interface between salt and the surrounding sediments reflecting and refracting seismic energy along with velocity pull-up below the salt (Hudec and Jackson, 2007). The velocity pull-up observed at both study areas. Interpretation of the salt structures performed with information of velocity pull-up below the salt and results from seismic attributes study for both area. Determining the base of the salt topography when it is visible is an useful tool to identify what type of salt system is present. In the Dan Field, the base of salt is visible in the study area (Figure 7.3 and 7.4). However, the base of the two salt structures is not recognizable along most of the study area in the Mars-Ursa Field (Figure 7.5 and 7.6).

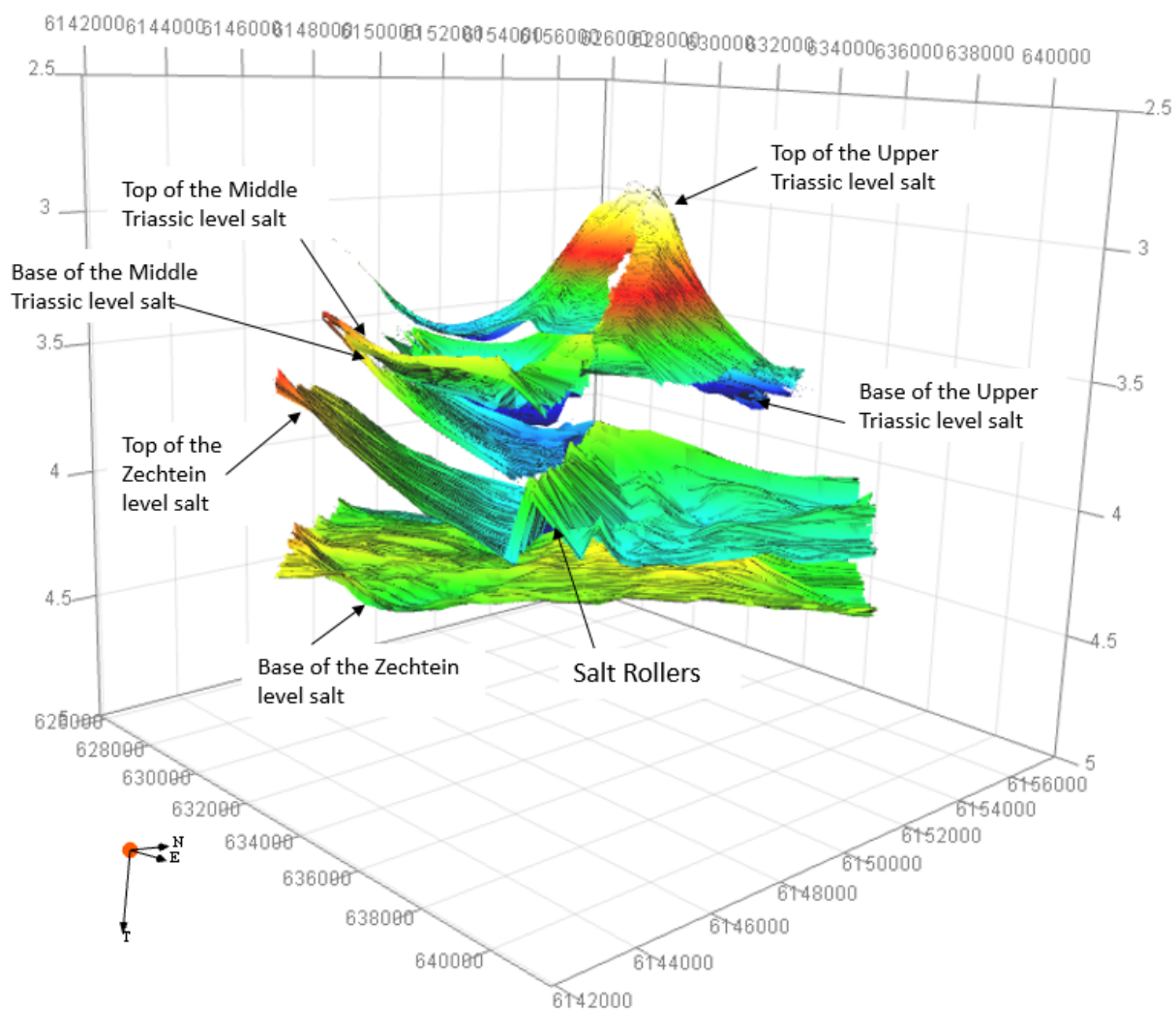


Figure 7.3. Three-dimensional visualization of salt distributions. Salt ridge of interpreted salt bodies in the Dan field.





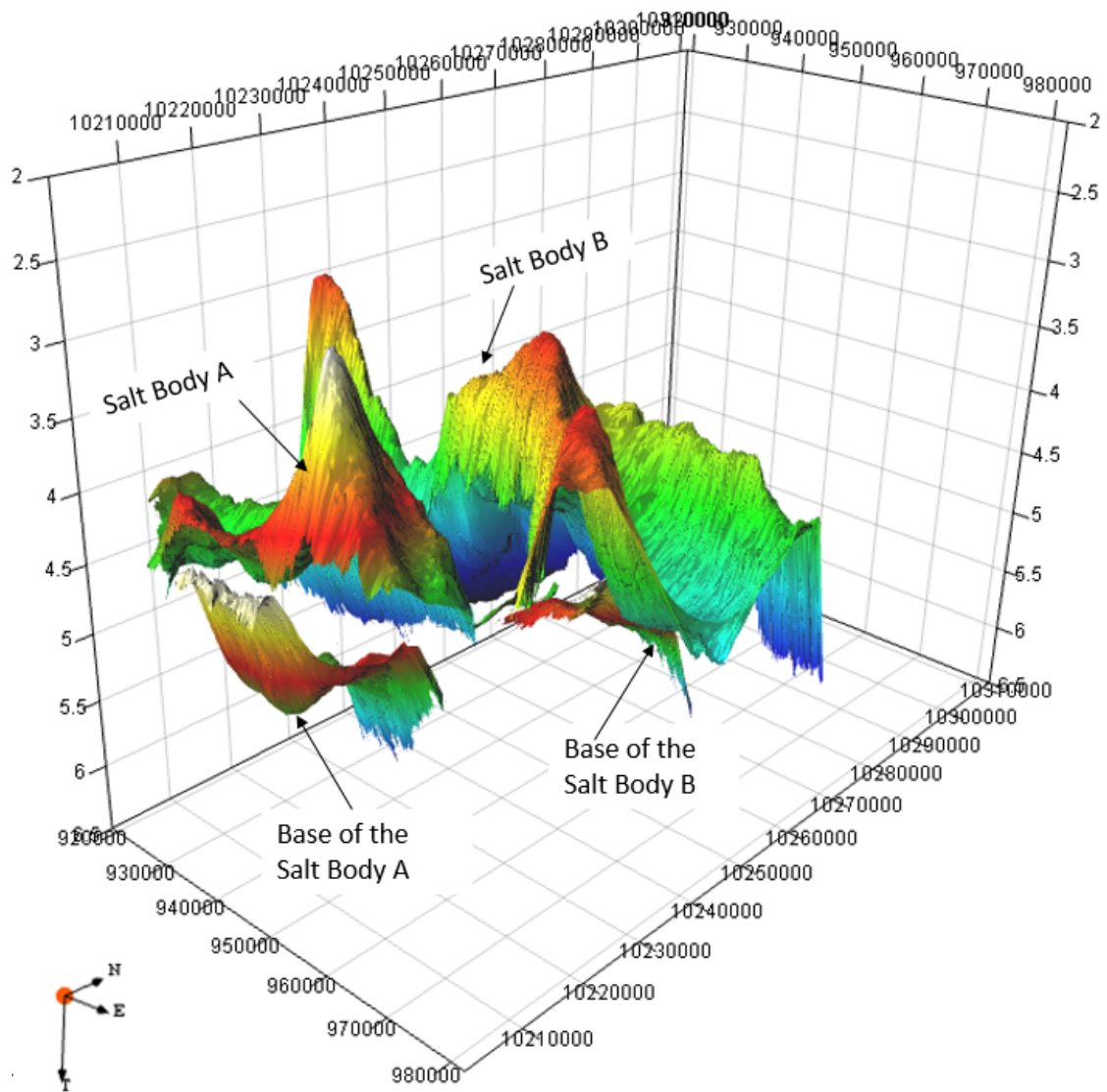


Figure 7.5. Three-dimensional visualization of salt distributions. Salt ridge of two interpreted salt bodies in the Mars-Ursa field.

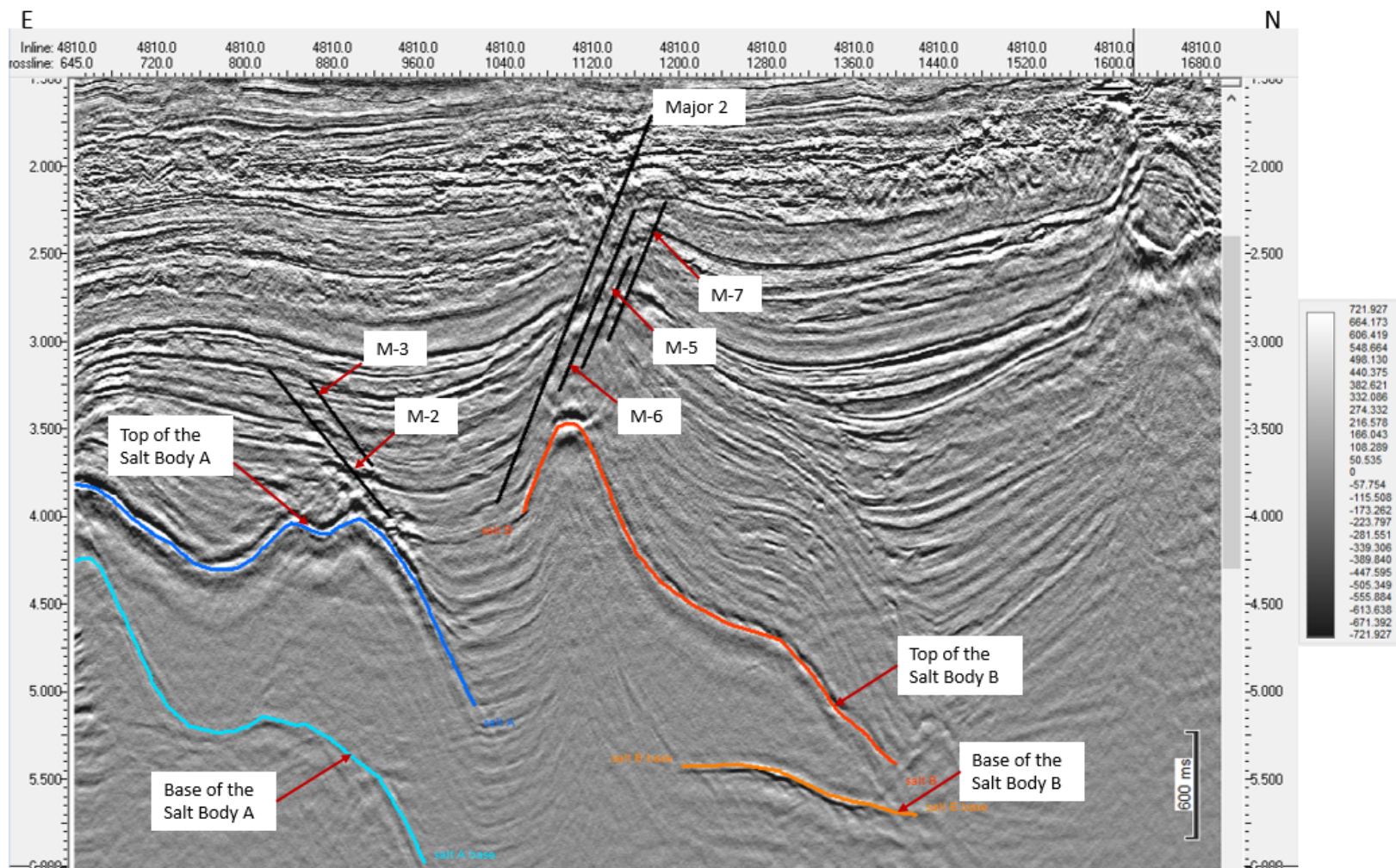


Figure 7.6. Vertical seismic section of the Inline 48100 shown interpreted salt bodies and faults.

## 8. RESULTS

### 8.1. DAN SALT STRUCTURE

The Dan Salt Structure reveals a complex geometry. The structure has an upper and lower parts. The evolution stage of the lower part is related to asymmetrically shaped Zechstein salt, while the upper part is influenced by salt at more than one different Middle-Upper Triassic stratigraphic levels (Jørgensen, 1992).

The upper part was interpreted as completely Triassic salt by Jørgensen (1992). However, an interpretation by Sundsbø and Megson (1993) demonstrates that the intra Triassic structure is composed of intruded Zechstein salt.

The strike slip model mentioned by Cartwright (1987) and Sundsbø and Megson (1993) suggests that the right and left lateral strike slip movement with related extension inclusive of the Dan Transverse Zone has influence on the Zechstein salt mobility and intrudes the overlaying Triassic age strata.

There is also another model that piercement location was controlled by intersected faults, which were located parallel to the graben, and crosscuts the transverse fault at basement level (Gaversen, 1994). According to this study, asymmetric salt was identified as a roller type salt structure within the NNW-SSE trending fault. A salt roller is defined as a low amplitude asymmetrical structure where one side of the salt body is bounded by a normal fault (Park, 1997). In the study area salt rollers are related with NNW-SSE trending normal fault and are recognized by their triangular shapes (Figures 8.1 and 8.2).

The intra Triassic salt bodies and underlying Zechstein salt are partially adjoining through the fault. According to Rank-Friend et al. (2004) even as Triassic salt is presented, it has to be carried by a primarily weak zone or surface along where the Zechstein salt has



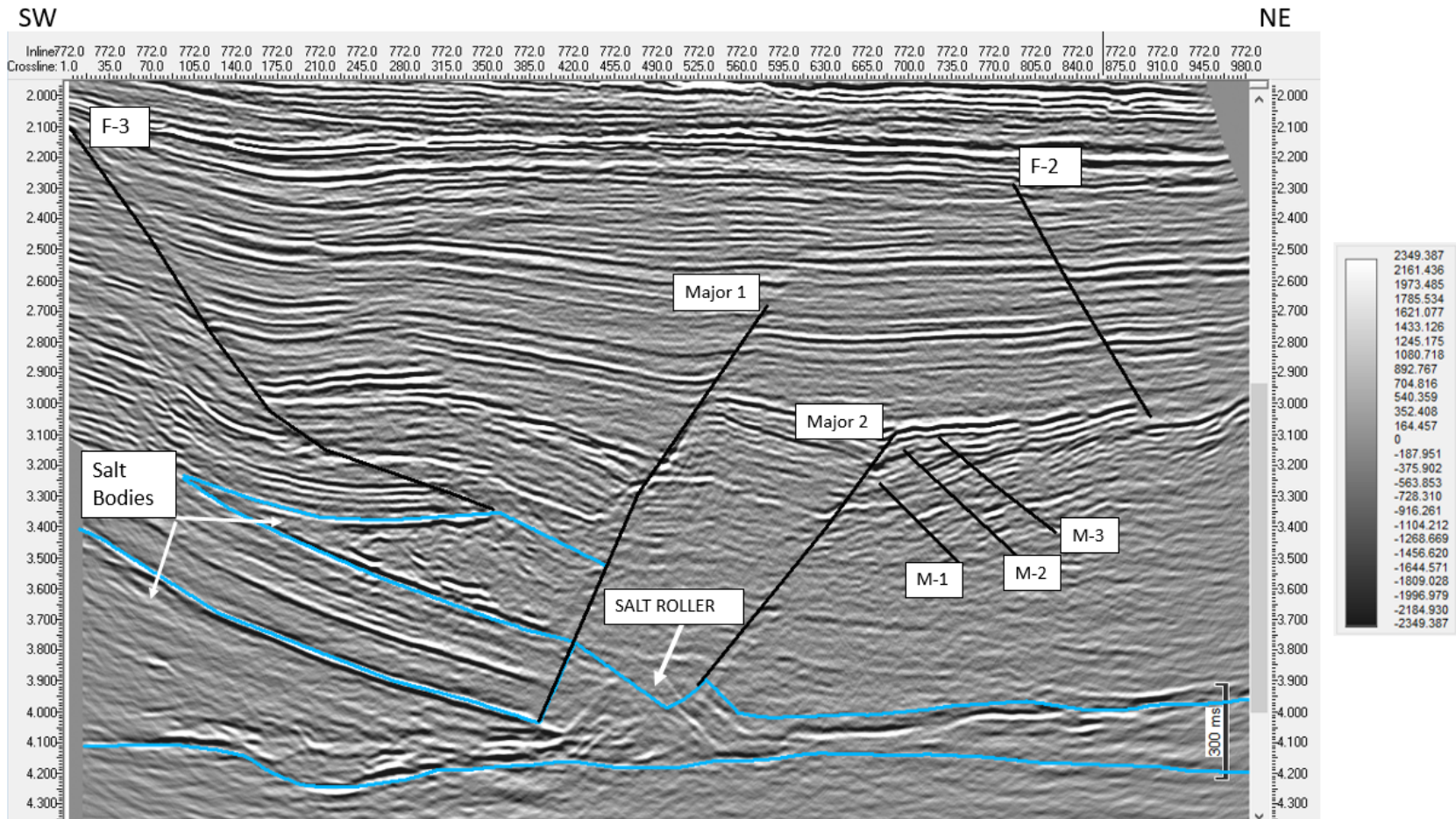


Figure 8.2. Vertical seismic section of Inline 772 shown interpreted salt bodies, faults, and salt roller type salt structure.

trespassed. While penetrated salt was not observed above the Triassic deposits, change in dimension and doming up to the overburden is widespread into the Eocene age, possibly influenced by Jurassic-Cretaceous sequences.

Evolution of the salt structure has influenced different geologic events over the time. It is suggested that extensional faulting is the primary reason which led to the top of the Triassic strata becoming thicker into an active fault during the Late Triassic growing stage of the interested part of the central graben (Rank-Friend et al., 2004).

During the evolution stages, a thick-skinned defined extension along the Coffee Soil Fault, which is located at eastern edge of the graben, and the formation of the N-S trending depocenter in its hanging wall took place.

Although it is not much clear, the Dan Salt Structure may have begun to form by itself at the same time as the Coffee Soil Fault phase. NE trends high with the present day location which is considered as an evidence. Salt development occurred around the Triassic age faults. The structural evolution throughout the Middle and Late Jurassic period was related to thick-skinned extension through eastward of the Central Graben. Consequently, two different depocenters were developed near the Coffee Soil Fault (Duffy et al., 2013).

The Dan Salt Structure is located in the current position and characterized by a similar decoupled extensional fault. Also, the faulting is associated with the growth of the salt structure. However, there was no salt mobility until Late Jurassic in the Dan Field area (Rank-Friend et al., 2004).

During the post rift in the Cretaceous, primary alteration in the morphological process of the salt structure occurred. Additionally, changes in the fault and depositional patterns took place. The Early Cretaceous was significant phase for the development of the Dan Salt Structure. It formed approximately as a circular outline during this time period (Withjack and Scheiner, 1982).

Significant salt migration took place in the Cretaceous time. This migration from NE to SE trending salt ridge is defined with Late Cretaceous within the Dan Salt Structure.

The salt formation was interpreted at three different stratigraphic levels which include the Zechstein, Middle Triassic, and Upper Triassic sections. Wedges of the salt became thicker and ended against the fault (Figures 8.3 and 8.4).

The underlying lower Triassic age strata was defined as parallel. Unformed sediment is stratigraphically proper with underlying Zechstein salt. The sequence over the Triassic age inner salt was faulted and folded around the salt bodies. Spreading of the Triassic age intra salt was specified as an elongated feature, settled primarily on the hanging wall of the NNW-SSE trending fault. The intra Triassic salt is interpreted at both part of the fault.

The seismic stratigraphy exhibits an isolated salt structure at a different level. However, evolution of salt structures in the Triassic strata occurred in itself from at the Zechstein level (Rank-Friend et al., 2004). Defining the interaction between intra Triassic and Zechstein salt distribution is complicated. Possibly, they juxtaposed at the other sides throughout the NNW-SSE trending fault. With this information, it can be assumed that the Zechstein salt intruded in a vertical direction along the weak horizon inside of the Mid-Upper Triassic sequences to generate an initial elongated NNW-SSE trending salt wall system. Additionally, this initially might have caused faulting in the Late Triassic. Yet, further growth and salt wall information was assisted by regenerated normal extension during the Mid-Late Jurassic rifting. Morphologic changes in salt structure occurred during the Cretaceous time and altered from regional extension to post rift thermal subsidence. Possibly, the Late Jurassic depocenter was not entirely loaded in the Early Cretaceous age and cause to unequal differential loading upon the salt layer ( Møller and Rasmussen, 2003). There is no evidence that salt migration paths were cut. However, further salt growth was prevented by cessation in thick- and thin-skinned extensional faulting. Cessation in this extensional faulting might be led to other mechanisms to be dominant. The growing of a domal circular outline possibly occurred during this process.





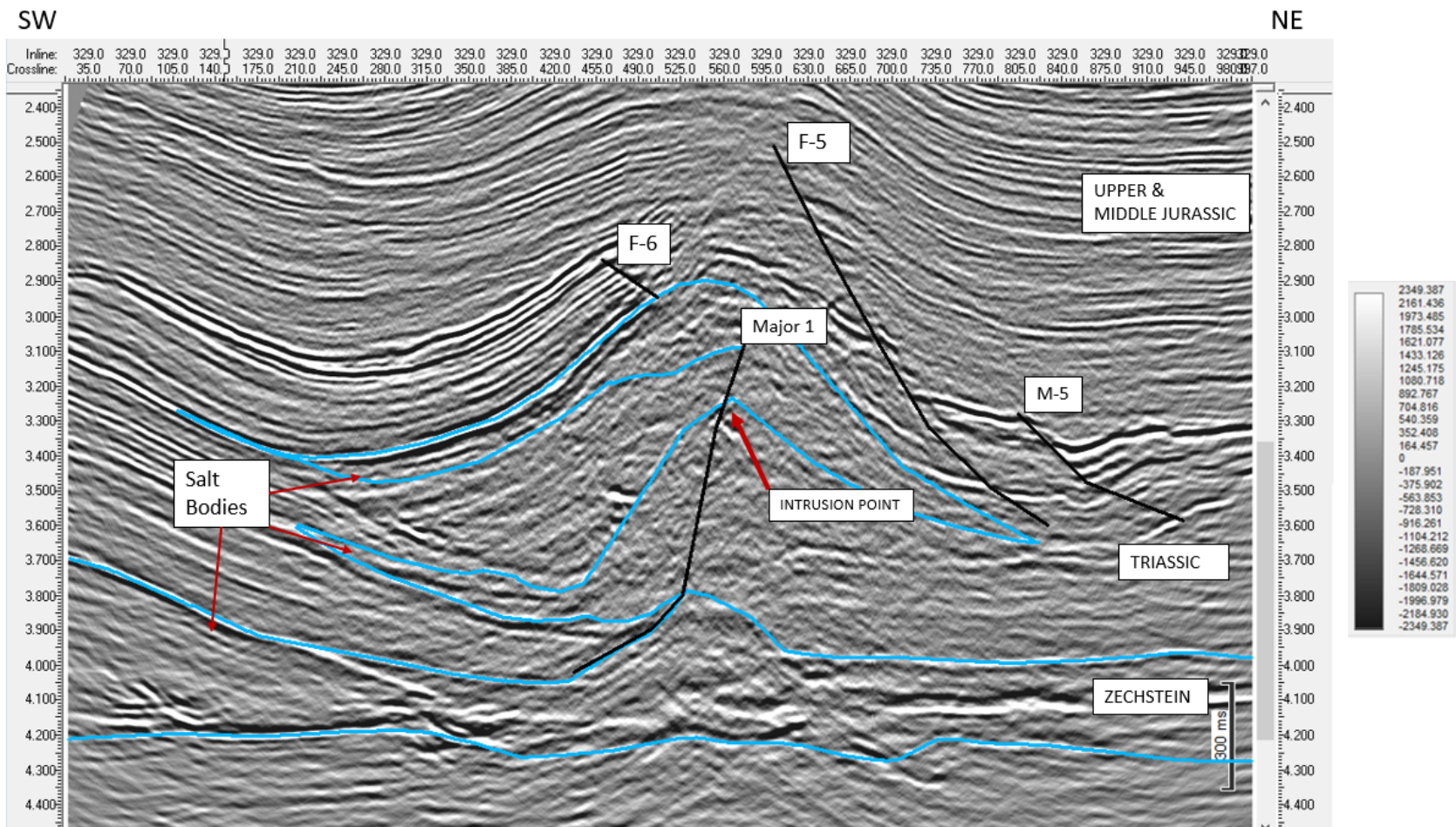


Figure 8.4. Vertical seismic section of Inline 329 shown interpreted salt bodies and faults.

This circular outline of growth is where the thin-skinned NW-SW and NNW-SSE faulting intersect within the Triassic and Jurassic sections. Further salt intrusion was controlled by weaker and thinner overburden that allowed bordered structural growth (Figures 8.5 and 8.6).

## **8.2. MARS-URSA BASIN**

The Mars-Ursa Basin is a salt withdrawal minibasin, and this minibasin is surrounded by allochthonous salt bodies. In this study, two salt bodies, i.e., Salt Body A and Salt Body B, were interpreted (Figure 8.7).

In the study area, the reflectors exhibit turtle geometry, which is shown as evidence for salt mobility. When an initial phase of salt mobility under a minibasin is followed by salt mobility around the minibasin, it results in turtle structure. Inverted minibasins are formed as a result of the collapse of minibasin flanks (Weimer et al., 2016). Basement structures and salt welds were not identified under the minibasins in the study area.

The deeper strata possibly have been affected by the Louann age autochthonous salt evacuation in the past. If any structure exhibited under the shallow salt bodies in the study area because of the poor subsalt seismic data quality, there is no structure identified in the study area.

A variety of sedimentation stage took place over the time, and the Mississippi River is defined as a primary source. In the minibasin, most Neogene aged sediment is identified as turbidites and classified as lowstand deposits (Martin et al., 2004). Glacia-eustacy and local tectonic activities also have significant impact on sedimentation stage. Sedimentation has been affected by salt movement and the evolutionary stage of surrounding salt system.

During the Early Miocene time, slow rate sediment accumulation took place in the Mississippi Canyon area. The depositional system is classified as the basin floor apron (Galloway et al., 2000).



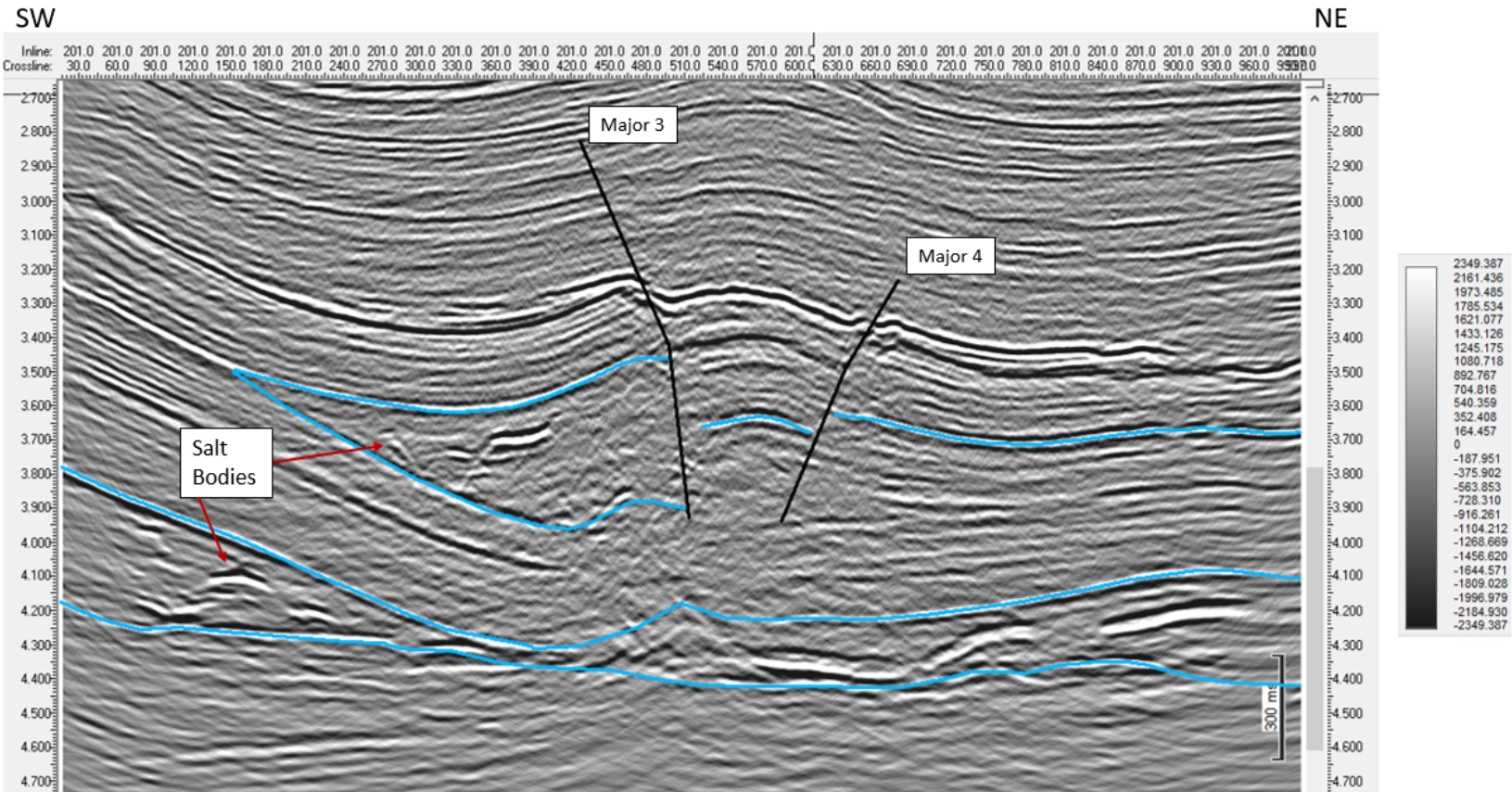


Figure 8.6. Vertical seismic section of Inline 201 shown interpreted salt bodies and faults.

The sedimentation rate in the southern Mississippi Canyon increased and was accompanied by salt mobilization and minibasin formation during the Middle Miocene. A large amount of sand was deposited during the Late Miocene, and this late sequence is dominated by slope fans in the Mars-Ursa Basin.

The salt system in the study area is defined as a part of counter regional salt system. In a counter regional salt system, the salt moves from the autochthonous salt layer to an allochthonous salt tongue, an unconformable salt body that intrudes obliquely into the overburden at the basinward limit of the salt layer. This term often refers to salt that is overthrusting the distal sediments at the basinward limit of the salt tectonic system, and then up into a shallower secondary diapir located basinward (Schuster, 1995).

These systems are formed in locations where thick source salt provided a high potential for accommodation for thick and extensive sediment wedges to form on the landward side of upward- and basinward-migrating salt. When the allochthonous salt was remobilized during the Neogene, minibasins were developed along the southward moving salt, triggering the formation of secondary allochthonous salt bodies (Hudec and Jackson, 2007).

These allochthonous salt bodies had seafloor expression and created slope perpendicular seafloor topography, which affected sediment gravity flow distribution. Sediments accumulated in geographically restricted ponded zones behind the salt bodies, rather than bypassing and being deposited farther basinward. Consequently, thick sediment wedges formed landward of the withdrawing salt, providing continued loading, evacuation, and upward and basinward movement of the salt. These salt systems only take place when the available amount of salt could no longer provide sufficient accommodation for sediment-gravity-flow sediment to accumulate.

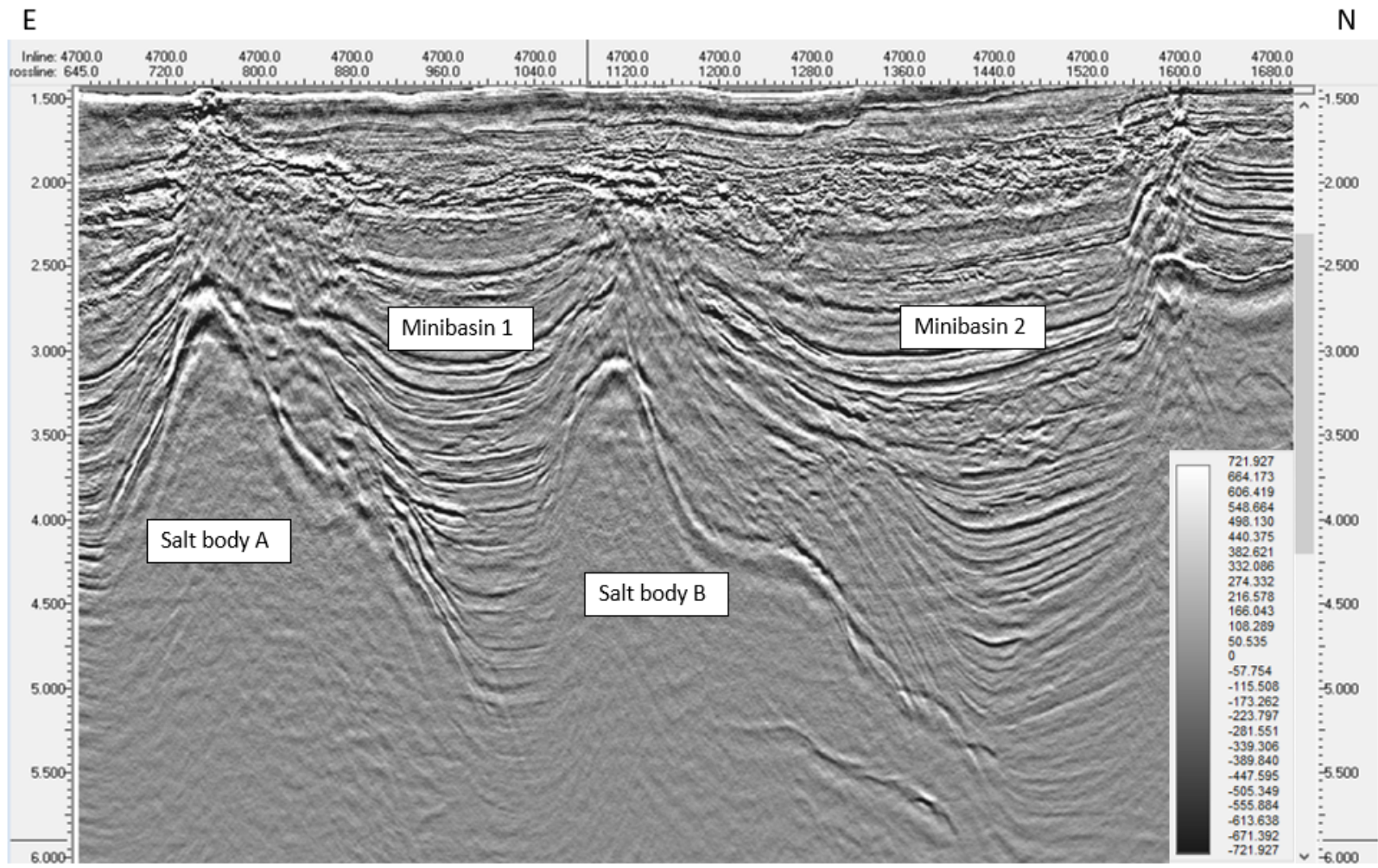


Figure 8.7. Vertical seismic section of Inline 47000 shown interaction between salt bodies and minibasins.

The original configuration of the autochthonous salt bodies onto which the counter regional salt systems developed controlled the type of allochthonous salt system that formed later. If the basal salt was thick and extensive, sediments could have accumulated in the form of thick, bowl-shaped or trough-shaped depocenters, which could have later inverted into symmetric or asymmetric turtle structures (Bouroullec and Weimer, 2017).

The counter-regional salt systems were oriented perpendicular to the regional sediment transport direction and locally influenced the sediment distribution pattern. The strike-oriented, salt-related topographic highs forced sediment gravity flows to be deflected and provided ponding geometries for the associated intra slope minibasins (Bouroullec and Weimer, 2017).

Salt withdrawal and rapid deposition occurred in the Mars-Ursa Basin during the Early Pliocene. Faulting in the study area is associated with salt diapirism. Suprasalt fault families are related to activity of underlying salt bodies. The area represents extensional faulting.

Reactive salt diapirism was observed in the study area at the eastern edge of Salt Body B (Figures 8.8 and 8.9). It shows E-W trending elongation, and is accompanied by normal faults and located along the updip edge of Salt Body B.

Either extension or differential loading can cause reactive diapirism (Jackson and Vendeville, 1994). Faults above these salt bodies are possibly crestal faults. The crestal faults are found above the salt bodies or folds and associated with local extension. Crestal fault families in a minibasin area possibly occur as a result of multidirectional salt evacuation (Rowan et al., 1999).

Active salt diapirism is also observed in the study area at the eastern edge of Salt Body A (Figures 8.10 and 8.11). The active diapirism is generally characterized by a salt top elevated above the regional datum. The active diapirism was accompanied by growth faults. Interaction between diapirism and faulting led to gas hydrate and assist to hydrocarbon movement from the subsurface to seafloor.

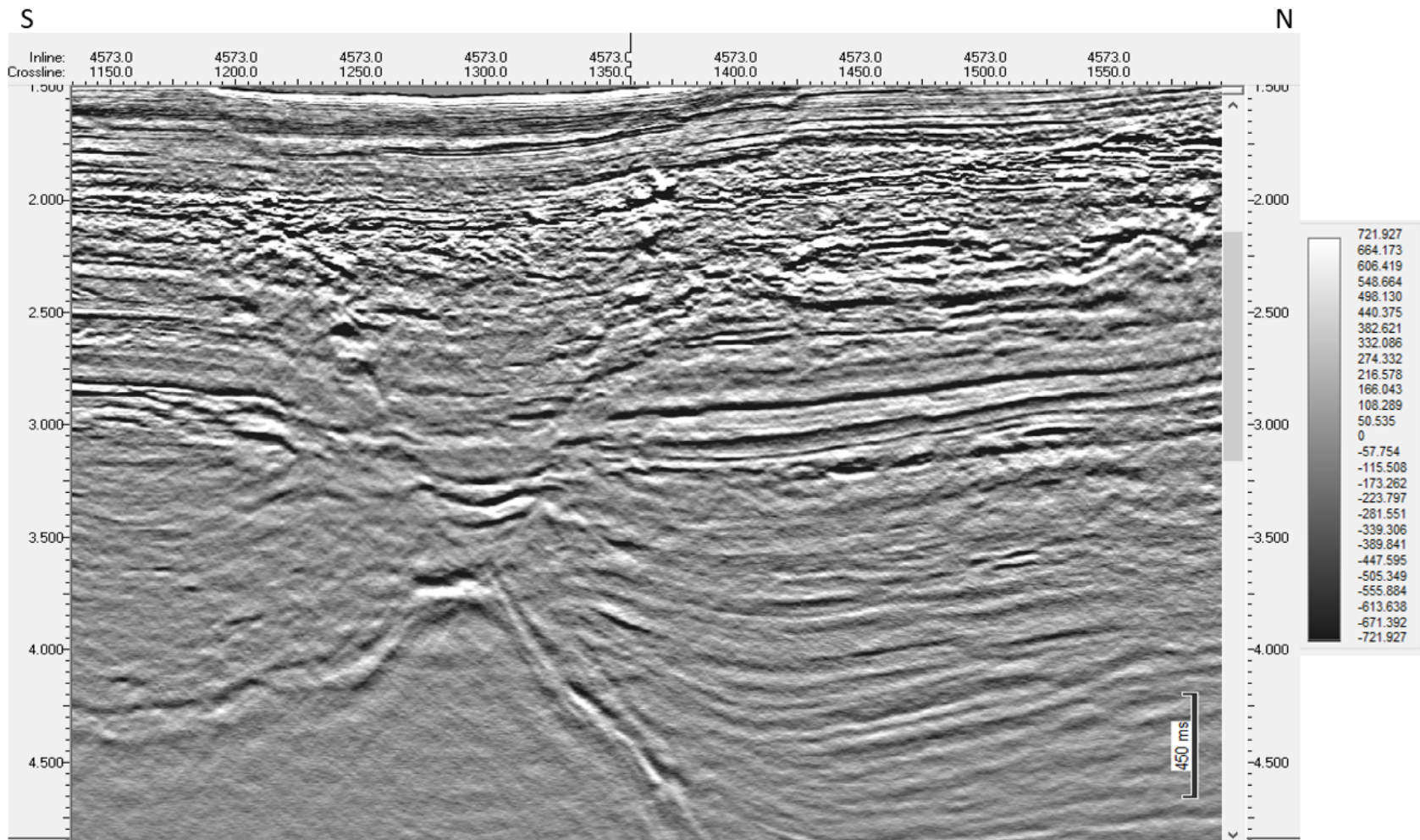


Figure 8.8. Vertical seismic section of Inline 4573 shown uninterpreted salt body and faults.



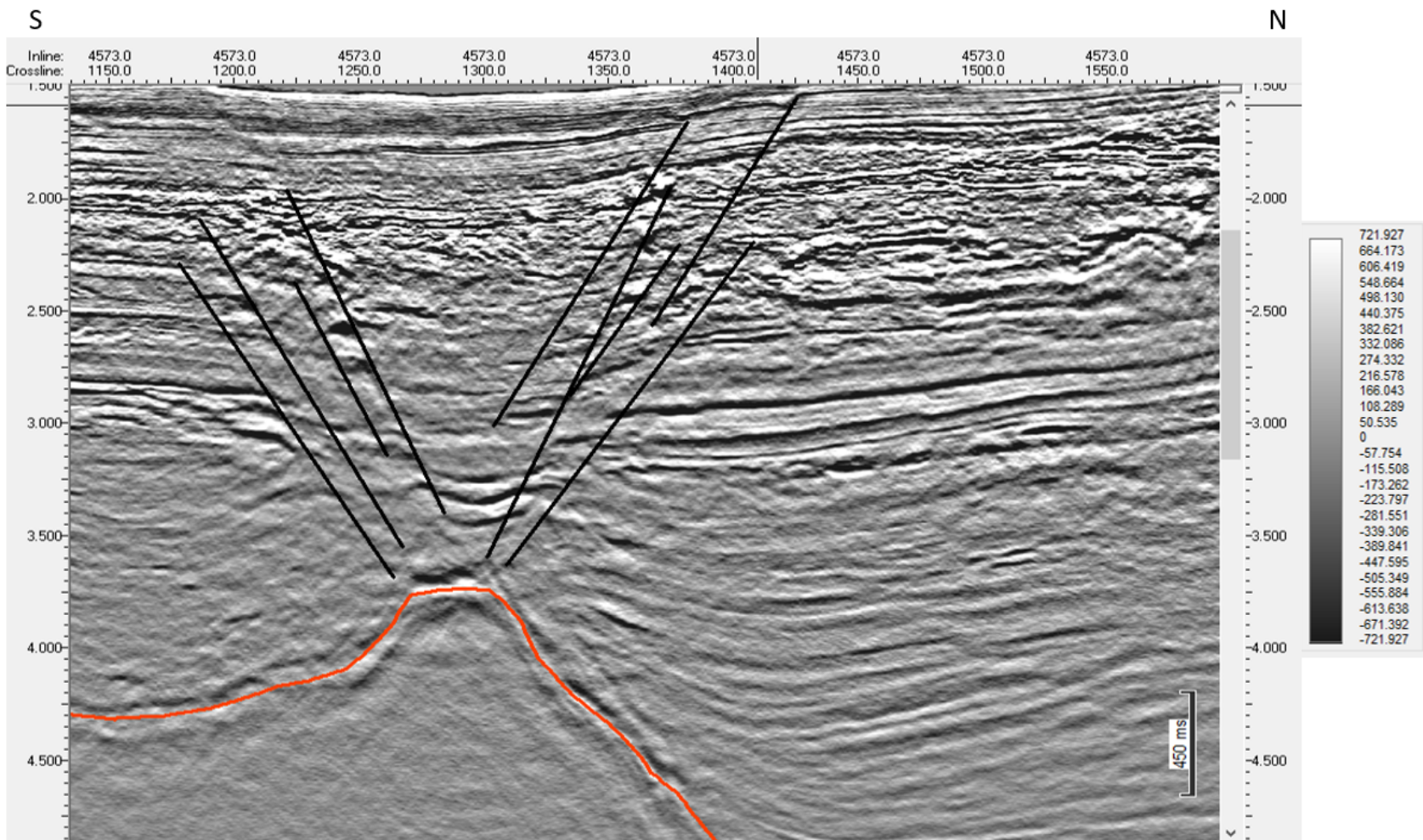


Figure 8.9. Vertical seismic section of Inline 4573 shown interpreted reactive diapirism and faults.

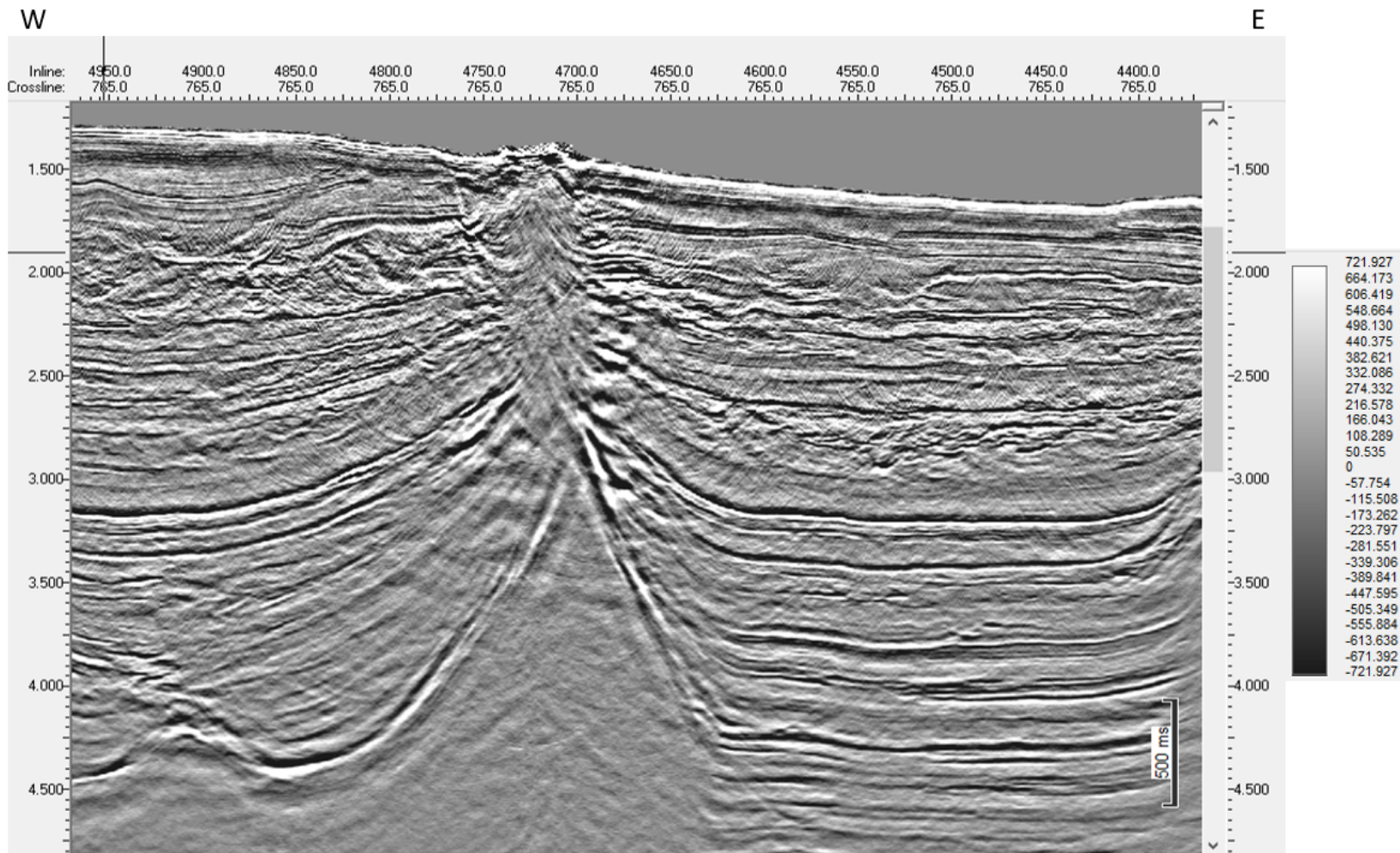


Figure 8.10. Vertical seismic section of Crossline 765 shown uninterpreted salt body and faults.

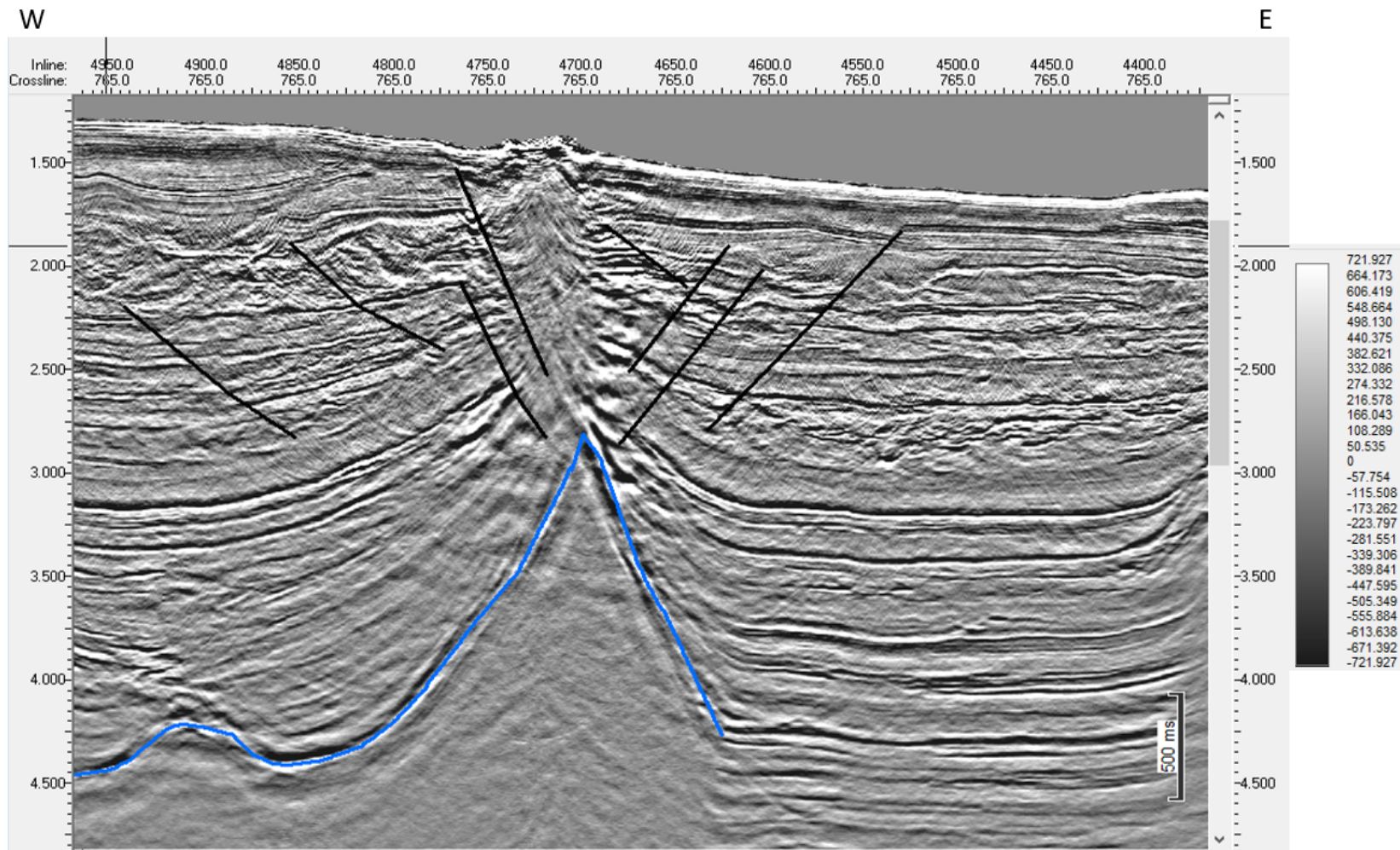


Figure 8.11. Vertical seismic section of Crossline 765 shown interpreted active diapirism and faults.

## 9. CONCLUSIONS

Although the evolution process of the Northern Gulf of Mexico and Danish Central Graben went through different geological regimes, the Dan Salt Structure and the Mars-Ursa Basin were influenced locally by regional extension. Regional extension and halokinesis have significant roles in structural development in both areas. The combination of the sedimentation, faulting, and mobilization of salt contributed to the growing process of the two areas.

The Dan Salt Structure was formed by uplifting a salt pillow from the Triassic age and it was subjected to various growth experiences from the Late Jurassic to the Late Tertiary. The structure was divided into upper and lower parts by NW-SE trending faults, also known as the Dan Transverse Zone. Extensional faulting is determined as a primary force for salt mobility. The Dan Salt Structure is interpreted as an asymmetric roller type salt structure within NNW-SSE faulting and salt bodies observed within three stratigraphic levels which are Zechstein, Middle Triassic, and Upper Triassic. The Dan Salt Structure is determined as a wall-and-sill complex.

The Mars-Ursa Basin is determined as a salt withdrawal minibasin and is formed by sediment accumulation during the Late Miocene to the Middle Pliocene. Sedimentation from N-NW during the Miocene loaded salt and triggered the evolution of the minibasin formation. The minibasin is surrounded by allochthonous salt bodies. Faulting in the minibasin is related to salt diapirism. Growth fault system is generally a common structure of the extensional system, resulting in gravity gliding above salt. During the stable tectonic conditions of the Cretaceous and Cenozoic time sediment loading stimulated the movement of Louann salt and development of growth faults. In the study area, active salt diapirism was observed at the eastern edge of Salt Body A. Active salt diapirism was accompanied by growth faulting and the elongation direction of diapirism, which was determined as

N-S. Reactive salt diapirism was observed at the eastern edge of the Salt Body B. Reactive diapirism was accompanied by normal faulting and elongation direction of diapirism, which was determined as E-W direction.

It is well known that regional extension plays a role in the evolution of diapirism. Most salt diapir provinces were started throughout phases of extension. Regional extension could result in active, reactive, and passive diapirism. While both areas underwent regional extension, in the Mars-Ursa minibasin, salt body movement ended with diapirism; however, salt movement beneath the Dan Salt Structure ended with wall-and-sill complex. The Dan Salt Structure has its own unique style instead of becoming diapiric. The possible explanation is with the growth stage of the Dan Salt Structure at this point, which was related to allocthonous movement in the Triassic strata, and was not able to pierce through the relatively thick, and competent overburden.

**BIBLIOGRAPHY**

- Allen, P. A. and Allen, J. R. (2013). *Basin analysis: Principles and application to petroleum play assessment*. John Wiley & Sons.
- Bird, D. E., Burke, K., Hall, S. A., and Casey, J. F. (2005). Gulf of Mexico tectonic history: Hotspot tracks, crustal boundaries, and early salt distribution. *AAPG bulletin*, 89(3):311–328.
- Bouroulllec, R. and Weimer, P. (2017). Geometry and kinematics of Neogene allochthonous salt systems in the Mississippi Canyon, Atwater Valley, western Lloyd Ridge, and western Desoto Canyon protraction areas, northern deep-water Gulf of Mexico. *AAPG Bulletin*, 101(7):1003–1034.
- Bouroulllec, R., Weimer, P., and Serrano, O. (2004). Salt tectonic history of the northeastern deep Gulf of Mexico.
- Buffler, R. T., Thomas, W. A., and Speed, R. (1994). Crustal structure and evolution of the southeastern margin of North America and the Gulf of Mexico basin. *Phanerozoic evolution of North American continent-ocean transitions: Geological Society of America DNAG Continent-Ocean Transect Volume*, pages 219–264.
- Cartwright, J. (1987). Transverse structural zones in continental rifts—An example from the Danish sector of the North Sea. In *Petroleum Geology of North West Europe*, volume 1, pages 441–452. Graham and Trotman London.
- Chopra, S. and Marfurt, K. (2007). Curvature attribute applications to 3D surface seismic data. *The Leading Edge*, 26(4):404–414.
- Chopra, S. and Marfurt, K. J. (2008). Emerging and future trends in seismic attributes. *The Leading Edge*, 27(3):298–318.
- Clark, J., Cartwright, J., and Stewart, S. (1999). Mesozoic dissolution tectonics on the west central shelf, UK central North Sea. *Marine and Petroleum Geology*, 16(3):283–300.
- Clark, J., Stewart, S., and Cartwright, J. (1998). Evolution of the NW margin of the North Permian Basin, UK North Sea. *Journal of the Geological Society*, 155(4):663–676.
- Clarke, S. M., Burley, S. D., and Williams, G. D. (2005). A three-dimensional approach to fault seal analysis: fault-block juxtaposition & argillaceous smear modelling. *Basin Research*, 17(2):269–288.
- Clausen, O. R., Egholm, D. L., Andresen, K. J., and Wesenberg, R. (2014). Fault patterns within sediment layers overlying rising salt structures: A numerical modelling approach. *Journal of Structural Geology*, 58:69–78.

- Coleman, J. M., Roberts, H. H., and Bryant, W. R. (1991). Late quaternary sedimentation. *The Gulf of Mexico Basin: Boulder, Colorado, Geological Society of America, The Geology of North America*, pages 325–352.
- Coward, M. (1995). Structural and tectonic setting of the permo-triassic basins of northwest europe. *Geological Society, London, Special Publications*, 91(1):7–39.
- Diegel, F. A., Karlo, J., Schuster, D., Shoup, R., and Tauvers, P. (1995). Cenozoic structural evolution and tectono-stratigraphic framework of the northern gulf coast continental margin.
- Duffy, O. B., Gawthorpe, R. L., Docherty, M., and Brocklehurst, S. H. (2013). Mobile evaporite controls on the structural style and evolution of rift basins: Danish central graben, north sea. *Basin Research*, 25(3):310–330.
- Erratt, D. (1993). Relationships between basement faulting, salt withdrawal and late jurassic rifting, uk central north sea. In *Geological Society, London, Petroleum Geology Conference series*, volume 4, pages 1211–1219. Geological Society of London.
- Evans, D. (2003). *The Millennium Atlas: Petroleum Geology of the Central and Northern North Sea; [a Project of the Geological Society of London, the Geological Survey of Denmark and Greenland and the Norwegian Petroleum Society]*.
- Farmer, P., Miller, D., Pieprzak, A., Rutledge, J., and Woods, R. (1996). Exploring the subsalt. *Oilfield Review*, 8(1):50.
- Fleet, A. J. and Boldy, S. (1999). Petroleum geology of northwest europe: Proceedings of the 5th conference. Geological Society of London.
- Fletcher, R. C., Hudec, M. R., and Watson, I. A. (1995). Salt glacier and composite sediment-salt glacier models for the emplacement and early burial of allochthonous salt sheets.
- Fossen, H. (2010). Structural geology, 463 pp.
- Galloway, W. E. (1998). Siliciclastic slope and base-of-slope depositional systems: component facies, stratigraphic architecture, and classification. *AAPG bulletin*, 82(4):569–595.
- Galloway, W. E., Ganey-Curry, P. E., Li, X., and Buffler, R. T. (2000). Cenozoic depositional history of the gulf of mexico basin. *AAPG bulletin*, 84(11):1743–1774.
- Gatliff, R., Richards, P., Smith, K., Graham, C., McCormac, M., Smith, N., Long, D., Cameron, T., Evans, D., Stevenson, A., et al. (1994). United kingdom offshore regional report: the geology of the central north sea. *British Geological Survey*.
- Giles, K. A. and Rowan, M. G. (2012). Concepts in halokinetic-sequence deformation and stratigraphy. *Geological Society, London, Special Publications*, 363(1):7–31.

- Glennie, K. and Buller, A. (1983). The permian weissliedend of nw europe: the partial deformation of aeolian dune sands caused by the zechstein transgression. *Sedimentary Geology*, 35(1):43–81.
- Glennie, K. W. (2009). *Petroleum Geology of the North Sea: Basic concepts and recent advances*. John Wiley & Sons.
- Gowers, M. B. and Sæbøe, A. (1985). On the structural evolution of the central trough in the norwegian and danish sectors of the north sea. *Marine and Petroleum Geology*, 2(4):298–318.
- Graversen, O. (1994). Interrelationship between basement structure and salt tectonics in the salt dome province, danish central graben, north sea. *Salt Tectonics. Petroleum and Tectonic Groups of the Geological Soc., Progr/abst*, pages 13–14.
- Gregersen, U. and Rasmussen, E. S. (2000). The subtle play-potential of upper jurassic–lower cretaceous block-faulted turbidites in the danish central graben, north sea. *Marine and Petroleum Geology*, 17(6):691–708.
- Gutiérrez, F. (2004). Origin of the salt valleys in the canyonlands section of the colorado plateau: Evaporite-dissolution collapse versus tectonic subsidence. *Geomorphology*, 57(3-4):423–435.
- Hodgson, N., Farnsworth, J., and Fraser, A. (1992). Salt-related tectonics, sedimentation and hydrocarbon plays in the central graben, north sea, ukcs. *Geological Society, London, Special Publications*, 67(1):31–63.
- Hossack, J. (1995). Geometric rules of section balancing for salt structures.
- Hudec, M. R. and Jackson, M. P. (2007). Terra infirma: Understanding salt tectonics. *Earth-Science Reviews*, 82(1-2):1–28.
- Hudec, M. R., Jackson, M. P., and Schultz-Ela, D. D. (2009). The paradox of minibasin subsidence into salt: Clues to the evolution of crustal basins. *Geological Society of America Bulletin*, 121(1-2):201–221.
- Jackson, M. and Talbot, C. J. (1991). *A glossary of salt tectonics*. Bureau of Economic Geology, University of Texas at Austin.
- Jackson, M. and Vendeville, B. (1994). Regional extension as a geologic trigger for diapirism. *Geological society of America bulletin*, 106(1):57–73.
- James, D. (1999). Glennie, kw (ed.) 1998. petroleum geology of the north sea. basic concepts and recent advances, xvi+ 636 pp. oxford: Blackwell science for japec (uk). price£ 44.95 (paperback). isbn 0 632 03845 4.-. *Geological Magazine*, 136(1):83–108.
- Johnson, R. and Dingwall, R. (1981). The caledonides: their influence on the stratigraphy of the northwest european continental shelf. *Petroleum Geology of the Continental Shelf of North-West Europe*. Heyden, London, 8597.



- Jorgensen, L. N. (1992). Dan field–denmark central graben, danish north sea.
- Klinkby, L., Kristensen, L., Nielsen, E. B., Zinck-Jørgensen, K., and Stemmerik, L. (2005). Mapping and characterization of thin chalk reservoirs using data integration: the kraka field, danish north sea. *Petroleum Geoscience*, 11(2):113–124.
- Konyukhov, A. (2008). Geological structure, evolution stages, and petroliferous complexes of the gulf of mexico basin. *Lithology and Mineral Resources*, 43(4):380–393.
- Mahaffie, M. (1995). Reservoir classification for turbidite intervals at the mars discovery, mississippi canyon block 807, gulf of mexico.
- Marillier, F., Eichenberger, U., Sommaruga, A., and Amphipôle, B. (2007). Seismic synthesis of the swiss molasse basin, report for 2007.
- Martin, J., Weimer, P., and Bouroullec, R. (2004). Sequence stratigraphy of upper miocene to upper pliocene sediments of west-central mississippi canyon and northern atwater valley, northern gulf of mexico.
- Megson, J. (1992). The north sea chalk play: examples from the danish central graben. *Geological Society, London, Special Publications*, 67(1):247–282.
- Møller, J. J. and Rasmussen, E. S. (2003). Middle jurassic–early cretaceous rifting of the danish central graben. *The Jurassic of Denmark and Greenland. Geological Survey of Denmark and Greenland Bulletin*, 1:247–264.
- Morley, C. (2007). Development of cretal normal faults associated with deepwater fold growth. *Journal of Structural Geology*, 29(7):1148–1163.
- Nelson, T. (1991). Salt tectonics and listric-normal faulting. *The Gulf of Mexico Basin: Geological Society of America, The Geology of North America, v. J*, pages 73–89.
- Pindell, J. L. (1985). Alleghenian reconstruction and subsequent evolution of the gulf of mexico, bahamas, and proto-caribbean. *Tectonics*, 4(1):1–39.
- Rank-Friend, M. and Elders, C. F. (2004). The evolution and growth of central graben salt structures, salt dome province, danish north sea. *Geological Society, London, Memoirs*, 29(1):149–164.
- Rowan, M. G., Hart, B. S., Nelson, S., Flemings, P. B., and Trudgill, B. D. (1998). Three-dimensional geometry and evolution of a salt-related growth-fault array: Eugene island 330 field, offshore louisiana, gulf of mexico. *Marine and petroleum geology*, 15(4):309–328.
- Rowan, M. G., Jackson, M. P., and Trudgill, B. D. (1999). Salt-related fault families and fault welds in the northern gulf of mexico. *AAPG bulletin*, 83(9):1454–1484.
- Rowan, M. G., Peel, F. J., and Vendeville, B. C. (2004). Gravity-driven fold belts on passive margins.

- Ruppel, C., Dickens, G., Castellini, D., Gilhooly, W., and Lizarralde, D. (2005). Heat and salt inhibition of gas hydrate formation in the northern gulf of Mexico. *Geophysical Research Letters*, 32(4).
- Salvador, A. (1987). Late triassic-jurassic paleogeography and origin of gulf of Mexico basin. *AAPG Bulletin*, 71(4):419–451.
- Salvador, A. (1991). Origin and development of the gulf of Mexico basin. *The gulf of Mexico basin*, pages 389–444.
- Sassen, R., Sweet, S. T., Milkov, A. V., DeFreitas, D. A., and Kennicutt, M. C. (2001). Thermogenic vent gas and gas hydrate in the gulf of Mexico slope: Is gas hydrate decomposition significant? *Geology*, 29(2):107–110.
- Satyavani, N., Sain, K., Lall, M., and Kumar, B. (2008). Seismic attribute study for gas hydrates in the Andaman offshore India. *Marine Geophysical Researches*, 29(3):167–175.
- Schuster, D. (1995). Deformation of allochthonous salt and evolution of related salt-structural systems, eastern Louisiana gulf coast.
- Sundsbo, G. and Megson, J. (1993). Structural styles in the Danish central graben. In *Geological Society, London, Petroleum Geology Conference series*, volume 4, pages 1255–1267. Geological Society of London.
- Taylor, J. and Glennie, K. (1998). Petroleum geology of the North Sea: Basic concepts and recent advances.
- Urai, J. L., Spiers, C. J., Zwart, H. J., and Lister, G. S. (1986). Weakening of rock salt by water during long-term creep. *Nature*, 324(6097):554.
- Van Bommel, P. P. and Pepper, R. E. (2000). Seismic signal processing method and apparatus for generating a cube of variance values. US Patent 6,151,555.
- van den Berg, A., Weimer, P., and Bouroullec, R. (2004). Structural evolution of the Mensa minibasin, Mississippi Canyon, northern deep Gulf of Mexico.
- Vejbæk, O., Frykman, P., Bech, N., and Nielsen, C. (2005). The history of hydrocarbon filling of Danish chalk fields. In *Geological Society, London, Petroleum Geology Conference series*, volume 6, pages 1331–1345. Geological Society of London.
- Vejbæk, O. V. and Kristensen, L. (2000). Downflank hydrocarbon potential identified using seismic inversion and geostatistics: Upper Maastrichtian reservoir unit, Dan field, Danish central graben. *Petroleum Geoscience*, 6(1):1–13.
- Warner, M. J., Elders, C., Davis, T., and Rank, M. (2002). Salt tectonics above complex basement extensional fault systems: results from 3D seismic analysis of central graben salt structures. In *American Association of Petroleum Geologists 2002 Annual Meeting Abstracts*, page 185.

- Warren, J. (1999). *Evaporites: their evolution and economics*. Wiley-Blackwell.
- Weimer, P. and Davis, T. L. (1996). Applications of 3-d seismic data to exploration and production.
- Weimer, P., Renaud Bouroullec, V. M., Adson, J., van den Berg, A., Lapinski, T., and Roesink, J. (2016). Petroleum geology of the mississippi canyon, atwater valley, western desoto canyon, and western lloyd protraction areas, northern deepwater gulf of mexico: Seals, source rocks, generation, and accumulation: Preliminary results.
- Withjack, M. O. and Scheiner, C. (1982). Fault patterns associated with domes—an experimental and analytical study. *AAPG Bulletin*, 66(3):302–316.
- Worrall, D. and Snelson, S. (1989). Evolution of the northern gulf of mexico. *The geology of North America; an overview: Geological Society of America*, v. A, pages 97–138.
- Wu, S., Bally, A. W., and Cramez, C. (1990). Allochthonous salt, structure and stratigraphy of the north-eastern gulf of mexico. part ii: Structure. *Marine and Petroleum Geology*, 7(4):334–370.
- Yapar, O. (2013). *Investigation of the interaction between salt movement, faulting and deposition, using high-resolution 3-D seismic data; Eugene Island South Addition, Gulf of Mexico*. PhD thesis.
- Zhang, Q., Chang, I., Li, L., et al. (2009). Salt interpretation for depth imaging—where geology is working in the geophysical world. In *2009 SEG Annual Meeting*. Society of Exploration Geophysicists.
- Ziegler, P. (1982). Triassic rifts and facies patterns in western and central europe. *Geologische Rundschau*, 71(3):747–772.
- Ziegler, P. (1990). Tectonic and palaeogeographic development of the north sea rift system. In *Tectonic evolution of the North Sea rifts*, volume 81, pages 1–36. Oxford Science Publications Oxford.
- Ziegler, P. and Van Hoorn, B. (1989). Evolution of the north sea rift system. In *Extensional tectonics and stratigraphy of the North Atlantic margins*, volume 46, pages 471–500. American Association of Petroleum Geologists.
- Ziegler, P. A. (1992). Plate tectonics, plate moving mechanisms and rifting. *Tectonophysics*, 215(1-2):9–34.

## VITA

Oznur Surek was born in Kesan, Edirne, Turkey. She received her B.Sc. degree in June 2013 in Geophysical Engineering at Istanbul University. She completed an internship in Turkish Petroleum Corporation in Ankara, and Gaziantep, Turkey in 2012. She was awarded a M.Sc. scholarship in 2014 from Turkish Petroleum Corporation. She studied at Rice University in English as a second Language Program from January 2015 to June 2015 in Houston, Texas. She started her Master of Science in the Geology and Geophysics department at Missouri University of Science and Technology in September 2016. During her graduate studies, she worked on salt mobility under different geological regimes. She received her M.Sc. degree in Geology and Geophysics at Missouri University of Science and Technology in December 2018.